Stony Brook University

Reconstructing Aquaporin 2 Trafficking and AHNAK Function in 3T3-L1 Adipocytes

A Dissertation Presented

by

Donne Bennett de Leon Caces

to

The Graduate School

in Partial Fulfillment of the Requirements

for the Degree of

DOCTOR OF PHILOSOPHY

in

Molecular and Cellular Pharmacology

Stony Brook University

May 2007

Stony Brook University

The Graduate School

Donne Bennett de Leon Caces

We, the dissertation committee for the above candidate for the

Doctor of Philosophy degree, hereby recommend

acceptance of this dissertation.

Jeffrey E. Pessin, Ph.D.
Advisor
William and Jane Knapp Professor and Chairman
Department of Pharmacological Sciences

Sidonie A. Morrison, Ph.D.
Chairperson of Defense
Associate Professor
Departments of Medicine and Pharmacological Sciences

Howard Crawford, Ph.D.
Assistant Professor
Department of Pharmacological Sciences

Erwin London, Ph.D.
Professor
Department of Biochemistry and Cell Biology

This dissertation is accepted by the Graduate School.

Lawrence Martin
Dean of the Graduate School

Abstract of the Dissertation

Reconstructing Aquaporin 2 Trafficking and
AHNAK Function in 3T3-L1 Adipocytes

by

Donne Bennett De Leon Caces

Doctor of Philosophy

in

Molecular and Cellular Pharmacology

Stony Brook University

2007

Using the 3T3-L1 adipocyte cell system, this dissertation reports novel insights obtained regarding the trafficking and compartmentalization of aquaporin 2 and the biological function of AHNAK. AQP2 is a facilitative water channel expressed naturally in the renal collecting duct epithelium. When expressed in adipocytes, AQP2 is sorted in a compartment that is distinct from endosomal vesicles and the insulin-responsive GLUT4 storage compartment. Additionally, it displays cAMP-dependent translocation in a manner similar to its behavior in renal epithelial cells. After synthesis, AQP2 gains direct access to the cAMP-regulated compartment and acquires forskolin-responsiveness within 3 hours. This is in contrast to GLUT4, which undergoes a slow 6-9 hour biosynthetic sorting step before acquiring insulin-responsiveness. Altogether, these data

demonstrate that adipocytes are equipped with two different molecular sorting apparatuses to direct hormone-sensitive partitioning of GLUT4 and AQP2.

AHNAK is a ubiquitously expressed phosphoprotein that physically interacts with actin and is reported to be an Akt substrate in epithelial cells. A proteomic analysis of lipid raft fractions from adipocytes identified AHNAK as a potential player in insulin signaling and GLUT4 trafficking. During adipogenesis AHNAK is negatively regulated and redistributes from an intracellular localization to the plasma membrane. The association of AHNAK with the plasma membrane is dependent on cholesterol and is most prominent at sites of caveolar formations. This distinct peripheral distribution is independent of cortical actin but down-regulation of AHNAK using small interfering RNA can effectively disrupt the formation of a peripheral actin belt. In the context of insulin-stimulated GLUT4 exocytosis, downregulation of AHNAK can efficiently disrupt GLUT4 translocation in response to insulin without affecting the insulin signaling cascade leading to Akt activation. In conclusion, the study proposes that AHNAK in adipocytes is a structural protein that anchors cortical actin to plasma membrane caveolae. In this model, AHNAK, indirectly supports GLUT4 exocytosis by holding cortical actin in position even as insulin-induced actin reorganization is taking place to accommodate translocation of GLUT4-loaded vesicles.

DEDICATION

Thank you God for the strength to endure.

I dedicate this dissertation to.....

The Molecular and Cellular Pharmacology Graduate Students: it was a real blast!

Bintou Diouf, Jennifer Pfaffly, Giuseppe Procino and Claire Bastie: It was the best of times, it was the worst of times.

The Vinh Ho, Jerome Gualbert, Ilaria Zanardi, Robert Watson, Martinne Mirrione, Michael Feigin, Adebanke Olijide and Dumaine Williams: Thank you for keeping my sanity intact.

Roberto Jacinto, Cristina Rodriguez, Carmina Castro, Karsten Pilones, Jody Junia and Lyza Bandong: I wouldn't have made it without you.

M. Paterno: for giving me a reason to believe.

I apologize to all of my other friends whom I have not mentioned by name. I am truly indebted to you.

Finally, I would like to offer this dissertation to my family. To Ma and Dad whose unconditional love keeps me going in leaps and bounds, to Ate Deng, Kuya Josel, Che and Aloy for always believing, to Jared, Brix, Khaye, and all my nephews and nieces for adding color to my life, Tita Chelo, Aunty Beccai and Aunty Fe for helping me cope, Joy for keeping me grounded.

We look before and after,
And pine for what is not:
Our sincerest laughter
With some pain is fraught;
Our sweetest songs are those that tell of saddest thought.

- Percy Bysshe Shelle
Ode to a Skylark

TABLE OF CONTENTS

LIST OF ABBREVIATIONS

AC	adenylate cyclase
ADH	anti-diuretic hormone
AKAP	protein kinase A-anchoring proteins
aPKC	atypical protein kinase C
APS	adapter protein with Pleckstrin homology and Src homology 2 domains
AQP2	aquaporin 2
AS160	Akt substrate of 160 kiloDalton
ATP	adenosine triphosphate
BFA	brefeldin-A
BSA	bovine serum albumin
cAMP	cyclic adenosine monophosphate
CAP	Cbl-associated adapter protein
cDNA	complementary deoxyribonucleic acid
cGMP	cyclic guanosine monophosphate
COOH	carboxy (terminus)
DMEM	Dulbecco's Modified Eagle's Medium
EDTA	ethylene diamine tetraacetic acid
EEA1	early endosome antigen 1
EGFP	enhanced green fluorescent protein
EGTA	ethylene glycol tetraacetic acid
ER	endoplasmic reticulum
F-actin	filamentous actin

FK	forskolin
GGA	Golgi-localized gamma-ear-containing Arf-binding protein
GLUT4	glucose transporter 4
GPI	glycosylphosphatidylinositol
GSC	GLUT4 storage compartment
GTP	guanosine triphosphate
HEPES	4-(2-hydroxyethyl)-1-piperazineethanesulfonic acid
HSP	high speed pellet
IBMX	3-isobutyl-1-methylxanthine
IR	insulin receptor
IRS	insulin receptor substrate
LC/MS/MS	liquid chromatography / mass spectroscopy / mass spectroscopy
LSP	low speed pellet
MβCD	methyl-β-cyclodextrin
M6PR	mannose-6-phosphate receptor
MAPK	mitogen-activated protein kinase
MDCK	Madine-Darby canine kidney
NH	amino (terminus)
PAGE	polyacrylamide gel electrophoresis
PBS	phosphate buffered saline
PCR	polymerase chain reaction
PDK1	phosphoinositide-dependent-kinase 1
PI3K	phosphatidylinositol-3-kinase
PIKfyve	phospatidylinositol-3-phosphate 5-kinase
PIP3	phosphatidylinositoltriphosphate
PKA	protein kinase A
PM	plasma membrane
PTB	phospho-tyrosine binding

SDS	sodium dodecyl sulfate
SH2	Src homology 2
siRNA	small interfering ribonucleic acid
TfR	transferrin receptor
TGN	trans-Golgi network
VAMP2	vesicle-associated membrane protein 2
V_2R	vasopressin type 2 receptor
WT	wildtype

LIST OF FIGURES

ACKNOWLEDGEMENTS

This dissertation took body and form because of the support of Dr. Jeffrey Pessin, my advisor. Thank you and I will forever be grateful.

I would like to thank my dissertation committee for their guidance and expertise. Dr. Erwin London for always finding the time, Dr. Howard Crawford for answering questions born out of naiveté and Dr. Sidonie Morrison for the emotional support.

Thank you Dr. Stella Tsirka for being the number one student proponent. I will always appreciate your understanding, your unconditional support and your positive prodding.

My appreciation goes out to everyone in the Department of Pharmacological Sciences, especially to Beverly Campbell, who always has the students' best interests at heart.

Thank you to the past and present members of the Pessin Lab for all the assistance.

The studies presented in figures 2.9, 2.10 and 2.11 were done in collaboration with Dr. Giuseppe Procino from the University of Bari in Italy. Thank you Giuseppe for your support.

CHAPTER 1
HORMONE-REGULATED EXOCYTOSIS

Proteins and lipids targeted to the plasma membrane or destined for secretion into the extracellular environment are adapted to various types of transport vesicles that fuse with the plasmalemma during exocytosis. While some molecules default to a non-selective constitutive secretory pathway and are exported automatically shortly after synthesis, others are retained intracellularly in specialized storage compartments that can be mobilized in the presence of the appropriate stimulus. Hormone-regulated exocytosis refers to the recruitment of a retained pool of cargo-loaded secretory vesicles for fusion with the plasma membrane in response to signals generated by binding of hormone to its receptor. The cargo may be a soluble factor or an integral membrane protein equipped with a distinct set of sorting and trafficking signals encoded within its primary structure.

The maintenance of glucose and water balance in the body is contingent on the proper functioning of two hormone-regulated exocytic systems. Insulin, which is secreted by the pancreas in response to post-prandial elevation of plasma glucose, facilitates the clearance of sugar from the blood by inducing the translocation of the facilitative glucose transporter GLUT4 to the plasma membrane in skeletal muscle and adipose tissue. Deficiency of, or resistance to, the effects of insulin accounts for the majority of the dysregulation observed in patients with diabetes mellitus.

To maintain intravascular fluid volume and osmolyte concentration, on the other hand, the body relies on the action of vasopressin or anti-diuretic hormone

(ADH). ADH mobilizes the water channel Aquaporin 2 (AQP2) from intracellular compartments to the apical membrane in the epithelium lining the renal collecting ducts. In hyperosmolar states, ADH effects the increased reabsorption of water from the urine to keep the blood at the appropriate osmolarity. In a water-wasting disease state called diabetes insipidus, patients are unable to synthesize and secrete, or respond to vasopressin resulting in excessive thirst and micturition, electrolyte imbalances and dehydration.

Studies on the molecular machinery supporting these systems fall into two broad categories. One investigates the components of the signaling pathways activated by insulin and ADH and the other looks into the redistribution mechanics of GLUT4 and AQP2 in response to hormone stimulation. It is not difficult to presuppose that regulation of the latter category is operationally identical. There are reports suggesting that GLUT4 and AQP2 share similar trafficking signals that allow for differential sorting and intracellular retention in basal condition. Thus, what is deemed as two unique systems may really be the same machinery operating in separate cellular environments. To address this issue, one part of this dissertation will present data obtained from studying the sorting and trafficking of GLUT4 and AQP2 side by side using the 3T3-L1 adipocyte cell line.

The second part of this thesis expands our understanding of the role of lipid rafts in insulin-regulated GLUT4 exocytosis. Lipid rafts are cholesterol and sphingolipid enriched microdomains in the plasma membrane. The selective partitioning of effector molecules within these platforms represents one mechanism by which cell signaling specificity and fidelity are maintained. In a separate chapter, the results of a proteomic screen done on lipid raft fractions isolated from adipocytes will be presented. AHNAK, a putative, lipid-raft associated, Akt substrate will be introduced as a significant downstream effector of insulin signaling leading to GLUT4 exocytosis.

INSULIN SIGNALING AND TRANSLOCATION OF GLUT4

The Classical Pathway: Insulin mediates GLUT4 translocation by binding to a heterotetrameric membrane receptor composed of two identical α and two β subunits linked together by disulfide bonds (Figure 1.1). Hormone binding is thought to bring the α-subunits closer together, resulting in a conformation that allows the β-subunit to bind ATP and autophosphorylate (32). Phosphorylation of at least three tyrosine moieties in the intracellular catalytic domain of the β subunit is essential for promoting the receptor's kinase activity. The juxtamembrane autophosphorylation sites, on the other hand, form essential docking sites for the insulin receptor substrate proteins.

The insulin receptor substrate (IRS) family is composed of four closely related proteins (IRS1-4) and a distant homolog (Gab-1) characterized by a phosphotyrosine-binding (PTB) module that facilitates interaction with an activated insulin receptor (IR). When bound to insulin, the receptor phosphorylates IRS at specific tyrosine motifs to create docking sites for proteins

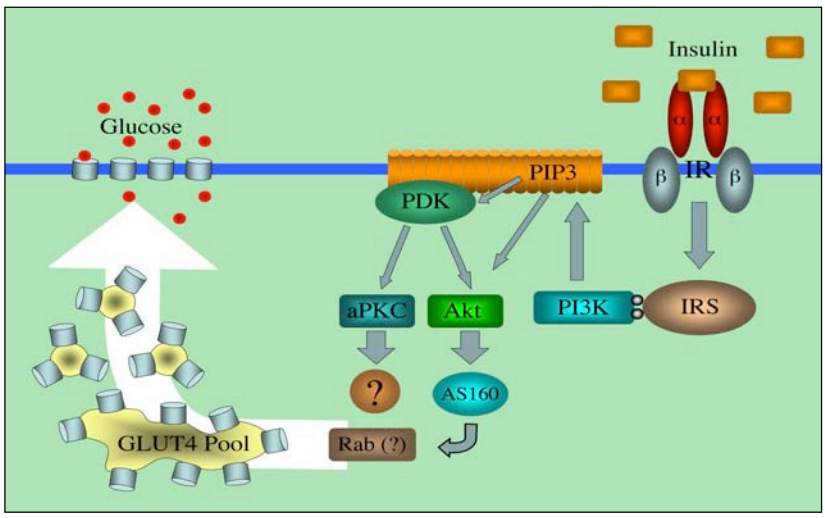

Figure 1.1 Schematic model of the classical pathway of insulin signaling involving the activation of phosphatidylinositol-3-kinase and Akt. Downstream of Akt and aPKC, the molecular effector/s that facilitate/s GLUT4 translocation is/are not entirely clear.

carrying a Src Homology 2 (SH2) domain (106). IRS-1 is believed to be the principal IRS in skeletal muscle while IRS-2 is thought to function primarily in the liver (55, 107). The overlapping tissue distribution of IRS proteins suggests that each isoform may subserve a specific set of functions. Genetic ablation studies in mice, however, have not implicated a specific type of IRS that is mostly responsible for the phenotype observed in clinical diabetes.

The tyrosine phosphorylation of IRS proteins generates docking sites for several downstream effectors including the p85 subunit of phosphatidylinositol 3-kinase (PI3K) (105). The interaction of the SH2 domain of p85 with phosphotyrosine motifs on IRS proteins brings the catalytic unit of PI3K (p110) adjacent to the plasma membrane where phospholipid substrates abound. PI3K catalyzes the phosphorylation of the 3' position in the inositol ring of phosphoinositol lipids generating phosphoinositol-(3,4,5)-triphosphate and phosphoinositol-(3,4)-bisphosphate. These lipid entities, in turn, recruit and activate proteins containing plekstrin homology domains including 3' phosphoinositide-dependent kinase-1 (PDK1) and Akt (16).

Akt or protein kinase B is believed to be the central mediator of glucose transport. Rapid activation of this serine/threonine kinase involves the phosphorylation of two key residues; threonine 308 is phosphorylated by PDK1 while serine 473 is modified by autophosphorylation (11, 12). Constitutively active Akt mutants are known to effect GLUT4 translocation in the absence of insulin while siRNA mediated ablation and dominant negative mutants result to inhibition of insulin-stimulated glucose uptake (41, 58). However, the exact Akt-regulated step/s in GLUT4 trafficking remain/s unclear. More than 30 Akt substrates have been identified to date but evidence for involvement in insulin-stimulated GLUT4 translocation is present for only two (104). AS160, a Rab-GTPase-activating protein containing five consensus sites for Akt phosphorylation, is believed to regulate the flux of GLUT4 containing vesicles

from an intracellular retained pool to the plasma membrane (69, 81). The recombinant GAP domain of AS160 can activate Rabs 2A, 8A, 10 and 14 which are all present in GLUT4-bearing vesicles (62). Precisely which Rab is involve in mobilizing GLUT4 and the exact mechanism by which it induces translocation are still unclear. Another substrate, PIKfyve, is the mammalian homologue of the yeast protein Fab1p involved in cargo sorting from late endosomes to lysosomes (85). In adipocytes, it is proposed to control the rate at which GLUT4 is sorted from internalizing endosomes back into the GLUT4 storage compartments (7).

Downstream of PI3K, atypical protein kinase C (aPKC λ/ζ) has also been implicated in insulin-dependent GLUT4 translocation. As with Akt, inhibition of aPKC using general inhibitors or expression of a kinase-dead or activation-resistant mutant inhibited GLUT4 translocation (4, 5). In contrast, expression of a constitutively active form promoted glucose transport (3).

The PI3-Kinase Independent Pathway: The existence of an alternative PI3K-independent pathway in adipocytes is suggested by studies showing that glucose uptake in cells pretreated with a PI3K inhibitor may be rescued by treatment with insulin and membrane permeant 3' phosphoinositide derivatives (39). In this pathway, the proto-oncogene c-Cbl, along with the adapter proteins CAP and APS, is recruited and phosphorylated by activated insulin receptors located within caveolin-enriched lipid raft microdomains (1, 64). Accumulation of the CAP/Cbl heterodimer in lipid rafts is facilitated by interactions with the resident caveolae protein flotillin (Figure 1.2). The resulting phosphotyrosine residues on Cbl provide docking sites for another protein complex composed of an SH2-containing adapter protein CrkII and C3G, a guanine nucleotide exchange factor capable of activating the GTPase TC10 (17). While the specific downstream effectors of TC10 remain uncertain, investigators propose that a possible mechanism for its regulation of insulin stimulated GLUT4 translocation is via

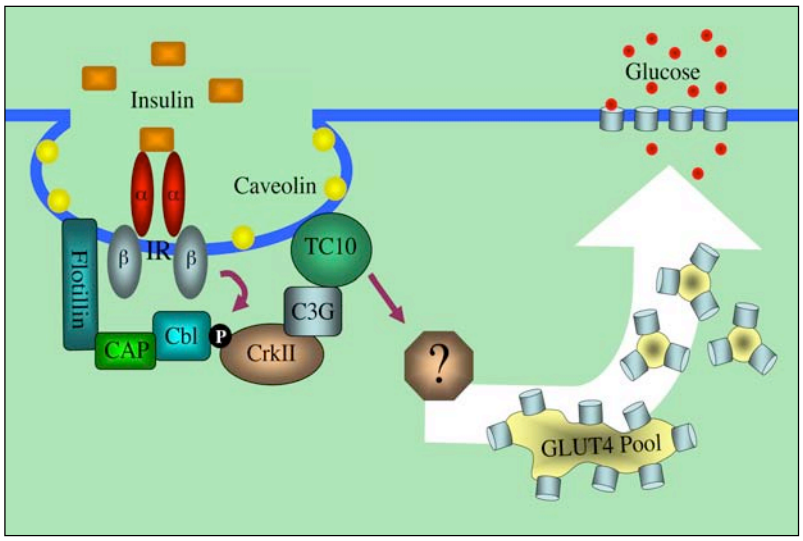

Figure 1.2 Schematic presentation of the alternative pathway of insulin signaling originating from caveolin-enriched microdomains and involving the proto-oncogene Cbl and the Rho familv GTPase TC10.

regulation of the cytoskeleton. This is not at all surprising because TC10, like Cdc 42 and Rac, is a member of the Rho family of small GTPases whose prominent effect is on the organization of the actin cytoskeleton. TC10 carries a CAAX targeting domain that is likely to be palmitoylated for appropriate targeting to lipid raft microdomains. Experimental mislocalization of TC10 into non-raft regions of the plasma membrane effectively curbs its ability to regulate GLUT4 translocation (103). In a recent report, insulin-activated TC10 was shown to recruit an exocyst complex composed of the proteins Exo70, Sec6 and Sec8. Targeted depletion of these proteins effectively blocks glucose uptake in adipocytes and it was proposed that exocyst assembly at lipid rafts is essential for the tethering of GLUT4-containing vesicles to the plasma membrane (33).

VASOPRESSIN SIGNALING AND TRANSLOCATION OF AQP2

The hormone vasopressin is released systemically from the posterior pituitary in response to an increase in serum osmolarity and a reduction in circulating blood volume. In the kidney, the hormone binds vasopressin receptors (V_2R) located on the basolateral membrane of the renal collecting duct epithelium (Figure 1.3). These receptors are coupled to the heterotrimeric G-protein G_s which turns adenylate cyclase (AC) on in response to hormone binding. Adenylate cyclase catalyzes the conversion of ATP to cAMP and leads to the activation of protein kinase A (PKA). When activated, PKA specifically phosphorylates AQP2 at serine 256 to facilitate translocation from intracellular storage compartments to the apical membrane (21, 53). Although the specific role of phosphorylation in

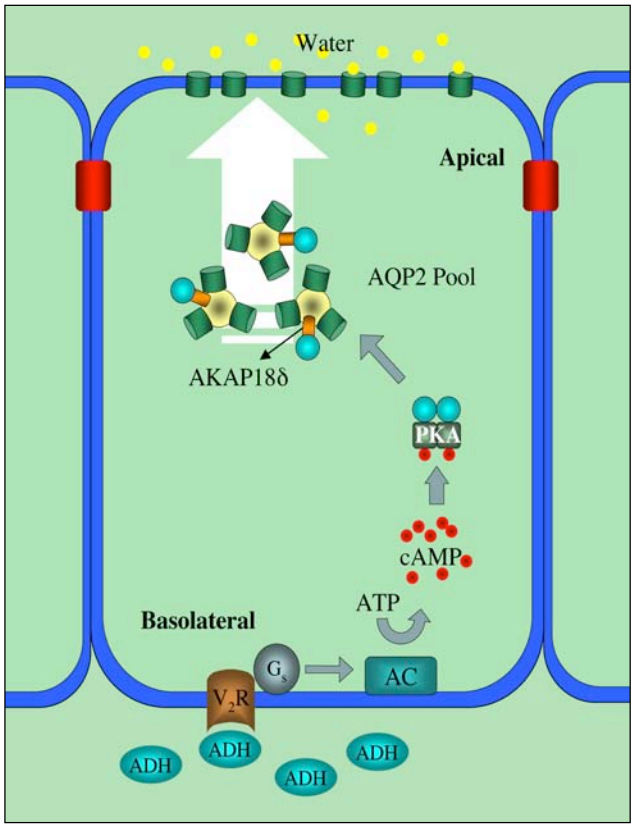

Figure 1.3 Schematic model of vasopressin or anti-diuretic hormone (ADH) signaling that leads to cell membrane recruitment of AQP2. The type 2 vasopressin receptors are located in the basolateral section of the polarized renal collecting duct epithelium. Phosphorylated AQP2 translocates to the apical side where it can facilitate reabsorption of water from the urine.

AQP2 trafficking is unclear, AQP2-bearing vesicles have been shown to contain PKA activity (61). This spatially-contained enzyme activity is facilitated by the protein kinase A anchoring protein AKAP18δ (28). At least three monomers in the AQP2 homotetramer need to be phosphorylated for the protein to be re-routed to the plasma membrane (43). The increase in water permeability resulting from the translocation of AQP2 allows water to flow from the urine in the collecting duct tubules back into general circulation.

Several groups have suggested that the unidirectional redistribution of AQP2 to the plasma membrane in the presence of vasopressin is made possible by the shuttling of AQP2-bearing vesicles along the cytoskeleton. In support of this model, specific inhibitors of dynein, an important element of the microtubular network known to associate with AQP2 vesicles, have been shown to inhibit the antidiuretic response in toad bladder (65, 66). Outside the microtubular system, reorganization of the apical actin network is documented to coincide with fusion of translocated AQP2 vesicles. Indeed, the current paradigm contends that F-actin depolymerization resulting from PKA-mediated inhibition of RhoA, the central mediator of actin oligomerization, is essential for appropriate docking and fusion of AQP2 vesicles with the apical membrane (94).

In addition to PKA, serine 256 is also a substrate for casein kinase 2 located within the Golgi apparatus. Phosphorylation of the serine residue at this location is necessary for sorting of AQP2 into vasopressin-responsive compartments (78). Phosphorylation motifs for protein kinase C and G are also present but their role, if any, in the regulation of the channel's trafficking remains unknown. Finally, as with GLUT4, alternative signaling pathways involving cGMP have been implicated in mobilizing AQP2, but whether PKA is also ultimately involved in these systems still remains to be addressed (10).

LIPID RAFTS IN HORMONE-REGULATED EXOCYTOSIS

The role of lipid rafts as signaling platforms is supported by studies demonstrating that many raft-associated proteins are involved in signal transduction. Mechanistically, raft domains are thought to facilitate signal amplification by concentrating downstream effectors and creating a microenvironment that is locally inaccessible to phosphatases and other negative regulators of signaling. In cases involving extracellular GPI-anchored signaling proteins where no transmembrane receptors are readily implicated, lipid rafts are thought to coordinate the inner and outer membrane leaflets to provide a link between the extracellular signal and the intracellular effectors (60).

Caveolae represent a subtype of lipid microdomains that are recognized as flask-like invaginations of the plasma membrane. These sphingolipid and cholesterol-rich structures are characterized by the presence of caveolin which is needed for the formation of caveolar pits. To date, three caveolin isoforms have been identified (caveolin-1, caveolin-2 and caveolin-3), with each type exhibiting a unique pattern of distribution. Caveolin-3 is expressed mostly in skeletal, smooth and cardiac muscle cells while caveolin-1 is expressed predominantly in adipocytes, fibroblasts and epithelial and endothelial cells (82, 96). Caveolin-2 closely follows the expression of caveolin-1 which has been shown to contribute to its stability (79). The involvement of membrane microdomains in hormone-regulated exocytosis and signal transduction, in general, is partly substantiated by the identification of signaling molecules that associate with immuno-isolated caveolae. A partial list of signaling molecules that have been shown to localize to, or reside within caveolae include Src family tyrosine kinases, G-protein coupled receptors and receptor tyrosine kinases (25, 63, 80).

Early evidence implicating caveolae in insulin signaling and GLUT4 trafficking came from studies done on 3T3-L1 pre-adipocytes where expression of

caveolin-1 is induced ~25 fold during differentiation into mature adipocytes. Caveolae isolated from these cells were shown to be highly enriched with the insulin receptor (25). When disrupted using cholesterol depleting agents such as β-methyl-cyclodextrin or overexpressing a dominant negative form of caveolin, insulin mediated IRS-1 phosphorylation, Akt activation and glucose uptake were abrogated without affecting other cellular functions (75). Careful analysis of the primary structure of the IR β-subunit revealed that the protein contains the characteristic caveolin-binding motif ϕ XϕXXXXϕ, where ϕ represents an aromatic ring (19). Interestingly, mutations within this motif have been identified in clinical studies involving patients with inherited severe insulin resistance and Type 2 diabetes (36, 70).

In addition to their role in insulin signaling, caveolae have also emerged as an important player in the actual targeting of GLUT4 to the plasma membrane. In the PI3K-independent pathway, the small GTP-binding protein TC10 has been shown to be constitutively localized within caveolar microdomains. As mentioned previously, experimental mistargeting by modifying specific membrane targeting domains blocks insulin-mediated activation of the G-protein and results to significant inhibition of glucose uptake. Additionally, TC10 binds specific components of the GLUT4 exocyst complex, suggesting that the protein may be important for docking and fusion of GLUT4 vesicles. This notion supports a model where GLUT4-bearing vesicles initially dock and fuse at lipid raft microdomains before transiting into non-raft regions (33). This model is supported further by studies demonstrating that insulin stimulation of adipocytes increases the amount of GLUT4 in caveolin-enriched membrane fractions (82).

The role of lipid rafts and caveolae in vasopressin signaling and AQP2 trafficking has not been as unambiguous as in the case of insulin and GLUT4. There are, however, studies involving other aquaporin isoforms that support a role

for membrane microdomains in the proper targeting and, perhaps, functioning of members of the aquaporin family. For instance, lipid rafts isolated from rat hepatocytes were shown to be enriched with AQP8 and AQP9 (67). Similarly, AQP1 was shown to be highly concentrated in caveolae isolated from rat endothelial cells and AQP5 in intracellular lipid rafts obtained from the rat parotid glands (35, 83). In terms of function, studies done on keratinocytes show that AQP3 forms signaling modules with phospholipase D2 on raft microdomains to enhance the synthesis of phosphatidylglycerol (109). In studies done on thymocytes, induction of apoptosis resulted to increasing association of AQP1 with caveolin-1, rendering the water channel inactive. The resulting decrease in cell volume reportedly facilitates adjustments in the intracellular concentration of potassium, creating the appropriate environment conducive for activation of apoptotic enzymes (37).

From the examples just cited, it is apparent that the creation of spatially restricted subdomains in the plasma membrane is integral to the proper functioning of hormone-facilitated exocytosis. Although the biochemical definition of lipid rafts, from their size and composition to their structure and lifetime, is still being debated, the biological relevance of membrane microdomains as signaling platforms is clear and undeniable. From this standpoint one can argue, that studies strategically designed to identify proteins associated with lipid raft microdomains may, in the end, also be expected to provide additional insights on how hormone-regulated systems function.

CHAPTER 2

COMPARATIVE ANALYSIS OF AQP2 AND GLUT4 COMPARTMENTALIZATION AND TRAFFICKING MECHANICS USING THE 3T3-L1 ADIPOCYTE SYSTEM

The regulated trafficking of hormone-responsive protein channels suggests the existence of specialized subcellular compartments from which a pool of transporters can be readily mobilized to translocate to the plasma membrane. Such a compartment has been characterized for the insulin-regulated transporter GLUT4 but has not been completely elucidated for the water channel AQP2. Current understanding of hormone-regulated trafficking dictates that these specialized compartments are the primary sites of hormonal action. While considerable progress has been made on understanding the signaling events that take place proximal to these storage pools, the direct effects of hormonal activation on these compartments remain a major unresolved issue. One engaging theory is that in the presence of insulin or vasopressin, a complex of accessory proteins assembles and modifies the interaction of GLUT4 and AQP2 cargo vesicles with the cytoskeleton leading to translocation to the cell surface. This model presumes that distinct targeting motifs are embedded in GLUT4 and AQP2's primary structure that will allow intracellular retention in basal condition and the recruitment of a unique molecular machinery to facilitate translocation in response to hormone stimulation. Previous studies have identified several motifs that may be important for GLUT4 and AQP2 trafficking. However, questions regarding the nature of the insulin and vasopressin-responsive compartments have not been totally addressed. For instance, it is still unclear whether the initial

sorting of GLUT4 and AQP2 from the Golgi is facilitated by identical sorting signals that recruit the same sorting apparatus. Further downstream, it remains unknown whether the insulin and vasopressin-responsive compartments are qualitatively similar even if expressed exclusively in separate cell systems.

The GLUT4 Storage Compartment

Existing data on the trafficking itinerary of GLUT4 suggest that, in basal condition, the transporter is engaged in two recycling pathways (Figure 2.1). The first cycle involves movement of a small but significant fraction of GLUT4 between the cell surface and the endosomal system. This bi-directional transfer explains the sustained presence of a small amount of GLUT4 at the plasma membrane even in non-stimulated states. The majority of GLUT4, however, is retained while in transit at recycling endosomes and eventually sorted into insulin-responsive GLUT4 storage compartments (GSCs). This cycle forming the 2nd pathway involves movement between endosomes, the TGN and GSCs (15).

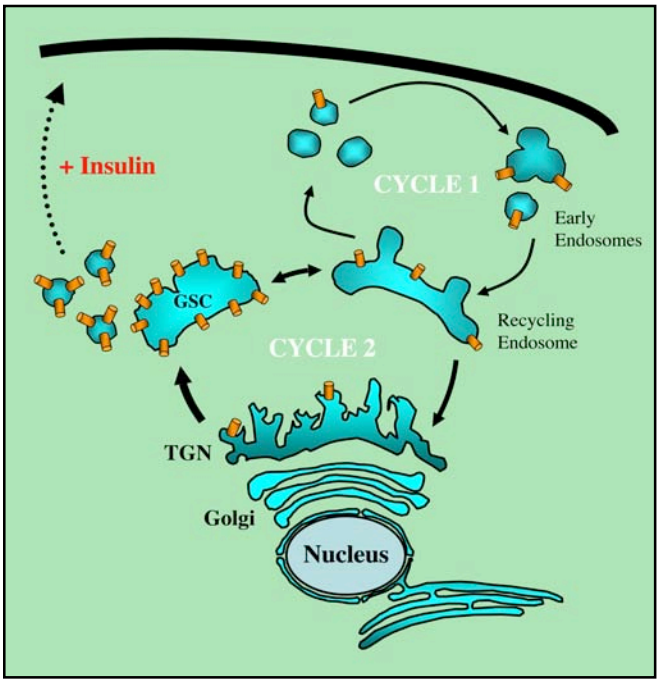

Figure 2.1. Schematic model of GLUT4's trafficking itinerary in insulin-responsive cells. Cycle 1 depicts movement of GLUT4 between the cell surface and endosome while cycle 2 illustrates shuttling between the TGN, endosome and GLUT4 storage compartment.

In the presence of insulin, GSCs are thought to move in a separate pathway that brings them directly to the cell surface. Attempts to characterize the GSC have shown that this secretory pool is composed of a discrete population of small vesicles that excludes other constitutively recycling proteins such as the transferrin receptor (TfR) and the mannose-6-phosphate receptor (M6PR) (27). Data is also present to suggest that this pool may be differentiated from more generic recycling vesicles by the absence of the protein cellugyrin (59). Without insulin, some vesicles from the insulin-responsive pool are thought to fuse slowly with endosomes, allowing a small fraction of GLUT4 to be targeted directly to the plasma membrane and to constitutively recycle using the endosomal network.

GLUT4 Targeting Motifs

The model described above predicts that GLUT4 contains intrinsic targeting domains that direct it to insulin-responsive compartments and allow it to be efficiently sequestered under basal conditions. Initial studies gathered evidence that a cytosolic N-terminal FQQI motif was important for intracellular sequestration. This was concluded after mutations done on the aromatic phenylalanine resulted in accumulation of GLUT4 at the plasma membrane (77). However, subsequent studies demonstrated that this effect is largely a consequence of faulty endocytosis rather than ineffective retention (2). Over time, more and more GLUT4 was targeted to and retained at the plasma membrane and this was wrongly interpreted as a result of aberrant retention.

In the same way, a dileucine (LL) motif within the cytoplasmic C-terminus of GLUT4 was initially implicated for intracellular sequestration, but later work showed that it functions more for endocytosis rather than basal retention (68). Unlike the FQQI motif, however, the LL motif was also reported in certain cell types to function during the exit of GLUT4 from the TGN, implying

that the same signal may be important at different stages of trafficking (88). Eventually, additional data was published showing that an acidic cluster (TELEYLGP) located downstream of the LL motif is also important for moving GLUT4 from endosomes to a subdomain of the TGN where it undergoes additional sorting processes before becoming insulin-responsive (84).

In more a recent study looking into the initial sorting of newly-synthesized GLUT4, it was shown that movement from the Golgi to insulin-responsive compartments requires the functional interaction of the NH-terminus and the large intracellular loop joining transmembrane domains 6 and 7 of the glucose channel (54). In addition, it was demonstrated that both the phenylalanine and the isoleucine residue of the FQQI motif were essential for this sorting event. This study supported the hypothesis that the same targeting motif may be functional at different stages of trafficking. More importantly, it opened a new avenue for research by delegating a more dynamic role for the large cytoplasmic loop connecting the two halves of the glucose transporter.

The AQP2 Storage Compartment

Characterization of the vasopressin-responsive AQP2 compartment has not been as thorough as it has been for the GLUT4 storage vesicles. Previous studies have shown that it is distinct from generic compartments like the lysosomes, the TGN and the ER (91). When overexpressed with GLUT4 in Madin-Darby Canine Kidney (MDCK) cell lines, AQP2 partitions to a separate compartment, suggesting that the two proteins carry non-identical sorting signals (92). In various publications, crude membrane fractions enriched with AQP2 and purified vesicles immunoadsorbed using AQP2 antibody have been used to identify other proteins that associate with the AQP2 compartments (42, 56). However, the nature of these isolated pools remains unclear because

characterization has been incomplete. In the case of GLUT4, for example, it has been established that the transporter subsists in two major compartments; one which is a derivative of the endosomal system and another which is unique and is able to respond to insulin stimulation. A similar understanding of AQP2 compartmentalization is currently lacking and it remains unclear whether vasopressin-responsive, AQP2-bearing vesicles in renal epithelial cells are entirely distinct from generic endosomes.

AQP2 Targeting Motifs

Phosphorylation of AQP2 at serine256 is crucial for membrane translocation in response to ADH. Shortly after synthesis, the channel exits the ER as a tetramer and in the presence of the hormone, at least three subunits have to be phosphorylated before translocation can take place (101). Interestingly, mutation of this residue only alters vasopressin responsiveness suggesting that other signals may be important in moving AQP2 between compartments.

AQP1 is an aquaporin isoform that is constitutively targeted to the plasma membrane. Analyses of the behavior of AQP1-AQP2 chimeras indicate that both the NH and COOH-termini are essential for targeting AQP2 to a separate compartment (99). A LL motif has also been mapped for the channel although, unlike GLUT4, the signal is situated within the sixth transmembrane domain of the protein making it unclear how it can participate in directing routing events (108). Downstream of this signal and right at the predicted start of the carboxy tail is an FPPA motif which has also been suggested to function like the FQQI motif of GLUT4. Like the LL motif however, more studies are needed to be able to designate a specific role for this putative signal.

In this study, the properties of both insulin-stimulated GLUT4 and PKA-stimulated AQP2 translocation was characterized and directly compared using the

3T3-L1 adipocyte cell line. The data presented will demonstrate that the cAMP-dependent plasma membrane translocation of AQP2 is facilitated by a signaling pathway that is completely separate from that activated by insulin. By showing that in adipocytes overexpressing both proteins, the AQP2-loaded compartments are spatially and functionally distinct from the GLUT4-bearing compartments, the study will provide credence to the notion that the cAMP-responsive AQP2 compartment is qualitatively different from the insulin-responsive GSC. In terms of sorting and trafficking dynamics, the study shows that newly-synthesized AQP2 rapidly acquires forskolin-responsiveness without transiting to the plasma membrane or undergoing endocytosis. Furthermore, the initial biosynthetic sorting of AQP2, in contrast to GLUT4, is shown to be independent of the function of the TGN adaptor protein GGA, suggesting that the water channel recruits a TGN sorting machinery distinct from that utilized by GLUT4. Collectively, these differences in compartmentalization and trafficking dynamics demonstrate that the vasopressin-regulated water channel recruitment described in renal epithelial cells and the insulin-regulated GLUT4 exocytosis characterized in muscle and adipose tissue are fundamentally different systems that most likely utilize a unique set of molecular effectors.

MATERIALS AND METHODS

Materials

FastPlasmid Mini-prep DNA kit was purchased from Eppendorf (Westbury, NY) and DNA gel extraction kits from Qiagen Inc. (Valencia, CA). Pfu Turbo Polymerase was obtained from Stratagene (La Jolla, CA) and Vectashield used for mounting microscopy specimens was purchased from Vector Laboratories (Burlingame, CA). All other chemicals used were obtained from Sigma (St. Louis, MO) unless otherwise specified.

Plasmids

The human wild type AQP2 cDNA was provided by Dr. Irene Konings from the University Nijmergen Medical Center, the Netherlands. The AQP2 cDNA was cloned in-frame into the EcoRI-NotI sites of the mammalian expression vector pcDNA3 obtained from Invitrogen. The previous construct was used as a template in overlapping polymerase chain reaction procedures to generate the AQP2-S256A and AQP2-S256D mutants. The forward sequences of the mutagenesis primers used for the PCR reactions are as follows: 5'-cgacggcggcag**acg**gtggag-3' for acquiring the AQP2-S256A mutant and 5'-cgacggcggcag**gac**gtggag-3' for acquiring the AQP2-S256D mutant. The forward primer 5'-gaattcgcccttgaatcgccaccatgtggg-3' and reverse primer 5'-gcggccgctaggccttggtacc-3' were used to introduce an EcoRI ant NotI site to facilitate subcloning into pcDNA3. The PCR products were cloned into Topo vector (Invitrogen), digested and subcloned into the pcDNA3 vector using the

same restriction sites. The final constructs were then sequenced in their entirety to ascertain that the appropriate mutations have been introduced. The human VAMP2 and EEA1 cDNA were inserted into the pEGFP-C1 vector (Clontech) using standard cloning techniques. The human transferrin receptor (TfR), c-terminal EGFP-tagged GLUT4 (GLUT4-EGFP) and myc epitope tagged GLUT4 (myc-GLUT4) constructs were prepared as previously described (34, 45, 97).

Culture and Transfection of 3T3-L1 Adipocytes

Murine 3T3-L1 pre-adipocyte cell line was obtained from the American Type Tissue Culture (ATCC) repository. Cells were maintained in Dulbecco's Modified Eagle's Medium (DMEM) supplemented with 25mM glucose, 10% bovine calf serum and 1% penicillin/streptomycin at 37°C and 8% CO_2. Two days post-confluency, differentiation into adipocytes was induced by shifting media into DMEM supplemented with 25 mM glucose, 10% fetal bovine serum, 1% penicillin/streptomycin, 1 μg/ml insulin, 0.25 μM dexamethasone and 0.5 mM 3-isobutyl-1-methylxanthine (IBMX). After 4 days, the same media less the dexamethasone and IBMX, was used to bathe the cells for 4 additional days. Fully differentiated adipocytes were used for transfection by electroporation using 100-150 μg of plasmid DNA under low voltage conditions (160 Volts, 950 microfarads). After electroporation, the cells were plated on collagen-coated glass coverslips and maintained in complete media to allow full recovery. Under these conditions, between 10 to 15% of cells efficiently expressed the encoded protein.

Indirect Immunofluorescence, Co-localization and Time-Course Experiment

Differentiated 3T3-L1 adipocytes transfected with the appropriate cDNA and expressing GLUT4-EGFP, wild type AQP2, AQP2/S256A or AQP2/S256D were grown on cover slips and serum-starved in DMEM for 2 h prior to each

experiment. For the co-localization studies, the adipocytes were co-transfected with 50 (g each of myc-GLUT4 and AQP2/WT cDNA, or 50 (g of AQP/WT and 50 (g of either EEA1-GFP, VAMP2-GFP or hTfR construct. The cells were then incubated with either insulin (100 nM) or forskolin (50 μM) for 30 min and the cover slips were processed for confocal microscopy. For the time-course experiments, stimulations were done at exactly 3, 6, 9, or 12 h after transfection. After each stimulation, the cells were fixed using 4% paraformaldehyde supplemented with 0.18% Triton X-100 for 20 min at room temperature and blocked using 1% BSA solution with 5% donkey serum for 1 h at room temperature. After blocking, the cover slips were incubated in primary antibody solution for 1 h at 37°C. The primary antibodies used were as follows: c-myc monoclonal antibody (Sigma), TGN38 sheep polyclonal antibody (Serotec), GM130 mouse monoclonal antibody (BD Transduction Lab), hTfR mouse monoclonal antibody (Molecular Probes) and AQP2-COOH rabbit polyclonal antibody. Each antibody solution is a 1:100 dilution of the stock (1-20 (g/ml) prepared in blocking solution. After incubation with the 1° antibody, the cover slips were washed three times with PBS and incubated in secondary antibody for another h at 37°C. The secondary antibodies used were as follows: anti-rabbit IgG Alexa Fluor 594 and anti-mouse IgG Alexa Fluor 488 (Molecular Probes). After incubation with the secondary antibody, the cover slips were washed with PBS and mounted on Vectashield Medium. PM translocation was determined by visualization on a Zeiss LSM510 confocal fluorescent microscope and scoring 50 representative cells/condition. The number of expressing cells displaying a continuous PM ring was calculated (mean ± SE) from 3-5 independent determinations.

RESULTS

GLUT4 and AQP2 are localized to distinct intracellular compartments when co-expressed in mature adipocytes.

The expression of GLUT4 in muscle and adipose tissue is totally separate from the expression of AQP2 in the principal cells of the epithelium lining the renal collecting duct. Because no cell naturally expresses both proteins, adipocytes, by virtue of their secretory nature, were tested for their capacity to provide the appropriate system to directly compare the sorting and trafficking of GLUT4 and AQP2. I initially examined the relative compartmentalization of the two proteins when co-expressed. To do this I co-transfected fully differentiated 3T3-L1 adipocytes with myc-GLUT4 and WT/AQP2 cDNA and studied their intracellular distribution by immunofluorescent microscopy. Under basal conditions, both proteins were localized primarily in the perinuclear region. A significant fraction of AQP2, however, was also scattered peripherally in punctate vesicles located in the cytoplasm and beneath the plasma membrane (Figure 2.2, panels a-c). Insulin stimulation resulted in robust translocation of GLUT4 but not AQP2 (Figure 2.2, panels d-f). Conversely, FK stimulated AQP2 translocation but not GLUT4 (Figure 2.2, panels g-i). Quantification of the relative extent of insulin and FK-stimulated GLUT4 and AQP2 translocation is shown in Figure 2.3.

To ensure that the apparent partial co-localization observed in the two-dimensional images in the XY plane were not a result of two separate compartments that were stacked on top of each other, the XZ and YZ images of representative cells were also reconstructed (Fig. 2.4A). In both insulin (Figure 2.4A-a) and FK-stimulated conditions (Figure 2.4A-b), AQP2 overlapped GLUT4

within the perinuclear region. These observations confirm that while AQP2 is retained in a distinct compartment in the cell periphery, part of its trafficking itinerary involves transit into a GLUT4-containing compartment. To further characterize this region of overlap, I compared the localization of GLUT4 and AQP2 with the cis-Golgi marker GM130 (Figure 2.4B, panels a-d) and the trans-Golgi marker TGN38 (Figure 2.4B, panels e-h). The fat arrows in figure 2.4B, panel d point to areas of overlap between GLUT4 and AQP2 that are distinct from GM130 localization. In contrast, the thin arrows in figure 2.4B, panel h point to areas where the green (GLUT4), red (AQP2) and blue (TGN38) signals overlap, suggesting that GLUT4 and AQP2 most likely cross paths while in transit at the trans-Golgi network.

Because AQP2 appears to localize to peripheral membrane compartments distinct from GLUT4, I compared the distribution of exogenous AQP2 with the early endosome marker EEA1, with transferrin receptor and with the SNARE protein VAMP2 (Figure 2.5). EEA1 displayed a punctate pattern that was poorly colocalized with AQP2 except at a few locations adjacent to the plasma membrane (Figure 2.5, panels a-d). Similarly, transferrin receptor, a membrane protein known to traffic using the generic endosomal system, was distributed peripherally throughout the cell but co-localized poorly with AQP2 (Figure 2.5, panels e-h). In contrast, VAMP2 extensively overlapped the peripheral AQP2-bearing vesicles underscoring the unique identity of these compartments (Figure 2.5, panels i-l).

The intracellular signals regulating AQP2 translocation in 3T3-L1 adipocytes are identical to renal epithelial cells.

To determine if the FK-dependent AQP2 translocation in adipocytes was facilitated by increases in intracellular cAMP levels, I tested the sensitivity and

responsiveness of AQP2 translocation to FK, isoproterenol, a cell permeable form of cAMP, 8-Bromo adenosine 3'5'-cyclic monophosphate (8-Br-cAMP) and the phosphodiesterase inhibitor 3-isobutyl-1-methylxanthine (IBMX) (Fig. 2.6). In all cases, I observed AQP2 translocation at agonist concentrations that induce or mimic physiologic increases in intracellular cAMP; isoproterenol (10nM-100 μM), IBMX (1μM- 1mM), FK (100 nM – 100 μM) and 8-Br-cAMP (1μM – 1 mM).

Several studies have also shown that hormone-regulated plasma membrane translocation is dependent upon cortical actin polymerization. In particular, depolymerization of cortical actin in adipocytes inhibits insulin-stimulated GLUT4 translocation (14, 50) but can potentiate cAMP-stimulated AQP2 translocation in renal epithelial cells (57, 93-95). As expected, depolymerization of adipocyte cortical actin with the actin monomer-sequestering agent, latrunculin B resulted in an inhibition of insulin-stimulated GLUT4 translocation (Fig. 2.7A). In contrast, latrunculin B treatment had no significant effect on FK-stimulated AQP2 translocation. The lack of potentiation probably reflects that at the dose of FK used, AQP2 translocation was already maximal.

TC10, is a Rho family member of GTP binding proteins that is suggested to play a role in the maintenance of cortical actin organization in adipocytes. It was previously shown that over expression of the mutant form of the protein can potently inhibit insulin-stimulated GLUT4 translocation (17). In the next study, I determined the effect of the GDP-bound dominant-interfering TC10/T31N mutant on AQP2 translocation (Fig. 2.7B). Consistent with previous findings, expression of TC10/T31N markedly inhibited insulin-stimulated GLUT4 translocation. In contrast, TC10/T31N had no significant effect on the FK-stimulated recruitment of AQP2 to the plasma membrane. Similarly, the dominant-interfering CAP mutant (CAPΔSH3) also inhibited insulin-stimulated GLUT4 translocation

without affecting FK-stimulated AQP2 translocation (Fig. 2.7C). To determine if PI3K has any role in the cAMP-regulated trafficking and recruitment of AQP2, adipocytes overexpressing either GLUT4 or AQP2 were treated with the PI3K-inhibitor wortmannin before stimulating with insulin or FK. As expected, insulin-stimulated GLUT4 translocation was completely inhibited by pre-treatment with wortmannin while FK-stimulated AQP2 translocation remained unaffected (Fig. 2.7D) (73). Together, these data demonstrate that adipocytes can fully support the regulated trafficking of AQP2 and GLUT4 through distinct intracellular localization and signaling pathways.

To further characterize the cAMP dependence of AQP2 translocation in adipocytes, the cellular distribution of wild type AQP2 (AQP2/WT), the S256A (AQP2/S256A) and S256D (AQP2/S256D) mutants was determined and compared (Fig. 2.8). In renal cells, the mutant with the alanine substitution at serine 256 mimics a constitutively non-phosphorylated or inactive state and is retained intracellularly. The aspartic acid substitution, on the other hand, mimics a constitutively phosphorylated state and creates a mutant that is expressed predominantly on the plasma membrane (100). Consistent with published data on epithelial cells, adipocytes expressing AQP2/S256A displayed a persistent intracellular localization of AQP2 that was unresponsive to forskolin (Fig. 2.8A, panels e-f). In contrast, the expressed AQP2/S256D protein defaulted to the plasma membrane in both the presence and absence of forskolin (Fig. 2.8, panels c-d). These data demonstrate that similar to renal collecting duct principal cells, cAMP-dependent serine 256 phosphorylation is sufficient to induce translocation of AQP2 to the plasma membrane.

Compared to GLUT4, newly-synthesized AQP2 more rapidly acquires hormone-responsiveness.

Having established that adipocytes can support the regulated trafficking of AQP2, I, in collaboration with Giuseppe Procino from the University of Bari in Italy, undertook several studies to examine and compare the trafficking itineraries of AQP2 and GLUT4. Our initial study investigated the time-dependent acquisition of forskolin-responsiveness of newly-synthesized AQP2. A recent report from our laboratory have shown that newly-synthesized GLUT4 undergoes a slow (6-9 h) biosynthetic sorting step before gaining access to the insulin-responsive storage compartment (54, 102). Consistent with these data, adipocytes acquired insulin-responsiveness between 6-9 hours following synthesis, with maximum response noted at 12 h after transfection (Fig. 2.9A). In contrast, forskolin-stimulated translocation of AQP2 was near maximal 3 h following biosynthesis, with no significant cell surface accumulation in basal state (Fig. 2.9B). These data demonstrate that newly-synthesized AQP2 undergoes a separate biosynthetic sorting step that is markedly faster compared to GLUT4.

Entry of newly-synthesized AQP2 into the forskolin-responsive compartment is not affected by inhibition of endocytosis.

In general, there are two pathways by which newly-synthesized AQP2 could gain access to its intracellular storage compartment. Following exit from the Golgi, AQP2 could default to the plasma membrane and undergo subsequent endocytosis and recycling to the cAMP-responsive compartment. Alternatively, AQP2 could be directly sorted to its storage compartment shortly after synthesis. Since AQP2 at the plasma membrane is recycled by clathrin and dynamin-dependent endocytosis (89), this issue may be addressed by studying forskolin-responsiveness in adipocytes where endocytosis is inhibited using a dominant-

interfering dynamin mutant. To do this, we transfected mature adipocytes with wild type (Dyn/WT) dynamin or the Dyn/K44A dominant-interfering mutant plus AQP2/WT and immediately treated the cells with Brefeldin A for 3 h. BFA blocks ER to Golgi anterograde trafficking and treatment after transfection will result to reversible accumulation of newly-synthesized AQP2 in the ER (78). However, since dynamin is a soluble protein, BFA treatment will not affect its ability to associate with the plasma membrane (102). After treatment, the cells were extensively washed and the time-dependent acquisition of FK-responsiveness was determined (Fig. 2.10). Under basal condition, expression of Dyn/WT did not affect the intracellular localization of AQP2 or the acquisition of FK-responsiveness that occurred by 3 h post-BFA washout (Fig. 2.10, solid circles and squares). In contrast, the expression of Dyn/K44A increased, in a time-dependent manner, the localization of AQP2 at the plasma membrane even in unstimulated cells (Fig. 2.10, open circles). Despite the slow plasma membrane accumulation, the expression of Dyn/K44A did not prevent the acquisition of FK-responsiveness which consistently peaked at 3 h (Fig. 2.10, open squares). Collectively, these data demonstrate that newly-synthesized AQP2 directly acquires cAMP-responsiveness without transiting the plasma membrane and undergoing endocytosis.

Dominant-interfering GGA mutant does not affect the entry of newly synthesized AQP2 to the forskolin-responsive compartment.

The Golgi coat/adaptor protein GGA plays essential roles in the TGN exit and sorting of several regulated proteins including GLUT4 and the M6PR. The protein consist of VHS domain that binds specific cargo proteins in the TGN, a GAT domain that binds Arf-1 and keeps the protein targeted to the TGN, a hinge domain that binds clathrin and a GAE domain that binds other accessory proteins.

As previously reported, expression of a dominant-interfering GGA mutant (VHS-GAT) completely prevents the acquisition of insulin-responsiveness of the newly-synthesized GLUT4 protein (102). Additionally, the VHS-GAT mutant also markedly reduces the basal state level of plasma membrane localization of GLUT4. To determine whether exit of AQP2 from the TGN is dependent on GGA, we determined the behavior of wild type AQP2 in the presence of VHS-GAT. The results of the study illustrate that expression of AQP2 with either the wild type GGA (red) or the dominant-interfering GGA mutant (blue) had no effect on the time dependent acquisition of cAMP-responsiveness of newly-synthesized AQP2 (Figure 2.11), further demonstrating that the initial biosynthetic trafficking of AQP2 is completely distinct from the sorting pathway utilized by GLUT4.

DISCUSSION

Hormone-regulated exocytosis is a well-orchestrated event that cells undergo to modify their surface or their immediate surroundings in response to changes in stimuli from the extracellular environment. This system is best exemplified by the insulin-regulated trafficking of the facilitative glucose transporter GLUT4 in muscle and adipose tissue (48) and the vasopressin-facilitated exocytosis of aquaporin 2 in renal collecting duct epithelium (13). In general, proteins that mediate their function on the cell surface enter the secretory pathway shortly after synthesis from the endoplasmic reticulum and transport into the Golgi apparatus (99). In the Golgi complex, further processing and maturation is facilitated by glycolipid and glycoprotein trimming enzymes that may provide the proteins with additional targeting signals to guarantee delivery into the appropriate destination (83). In the trans-Golgi network (TGN), the proteins are sorted and packaged into transport intermediates that will bring them directly to the plasma membrane or to specialized storage compartments that can readily exocytose in response to the appropriate stimulus (71). From the plasma membrane, these proteins may re-enter via early and recycling endosomes and then return to the same domain from which they originated (recycling) or to a different domain of the plasma membrane (transcytosis). In cell types that support hormone-regulated exocytosis, specialized storage pools may also originate from early endosomes and these compartments provide the ready supply of proteins that can be delivered to the cell surface in response to external stimuli.

In the absence of hormonal stimulation, GLUT4 and AQP2 undergo a slow but continuous recycling to and retrieval from the plasma membrane. At

steady state, the rate of endocytosis is significantly higher than the rate of exocytosis resulting into a net retention and intracellular sequestration of transporter units (24, 38, 52). Stimulation primarily results in an increase in the rate of exocytosis resulting in a new steady-state equilibrium that favors the cell surface membrane (38, 71). Following hormone withdrawal, exocytosis returns to a low rate and restoration of the basal steady-state distribution ensues. Since the endocytosed transporters are fully capable of undergoing subsequent rounds of stimulated exocytosis, it has been generally assumed that entry into these specialized storage compartments results exclusively from plasma membrane endocytosis. Although the plasma membrane recycling of GLUT4 into the insulin-responsive storage compartment certainly occurs, our laboratory have also previously demonstrated that newly-synthesized GLUT4 is directly sorted into this regulated compartment without first transiting the plasma membrane (102).

To identify a model system that can be utilized to directly compare the trafficking and sorting properties of AQP2 and GLUT4, adipocytes were tested for their capacity to provide the appropriate compartments and regulatory machinery to support cAMP-dependent AQP2 trafficking. When expressed in adipocytes, a fraction of AQP2 is localized to a perinuclear region that overlaps with GLUT4. However, a significant population of AQP2 is also positioned separately from GLUT4, scattered in small punctuate vesicles in the periphery that closely appose the plasma membrane. These AQP2-bearing compartments are mostly separate from endosomal vesicles, as evidenced by their minimal co-localization with the EEA1 marker and transferrin receptor, but partially co-localize with VAMP2. These data corroborate independent studies done on Madin-Darby canine kidney epithelial cells showing that AQP2 is retained in a distinct subapical compartment but utilizes the EEA1-positive early endosomal system shortly after retrieval from the plasma membrane (91). Moreover, the association with VAMP2-containing compartments is also consistent with the

established role of VAMP2 in AQP2 fusion with the plasma membrane in epithelial cells (72). In a broader sense, these data demonstrate that each protein is equipped with a unique set of targeting motifs that establishes the transporters trafficking itinerary and allow for functional segregation. Consistent with a distinct intracellular compartmentalization, elevation in cAMP levels by FK treatment effectively induces AQP2 translocation without significantly affecting the retention of GLUT4. Similarly, insulin stimulation mobilized the facilitative glucose transporter without perturbing the sequestration of AQP2. Analogous to renal epithelial cells, the translocation of AQP2 in adipocytes requires cAMP-mediated phosphorylation of serine 256 (21, 53). Altogether, these data demonstrate that not only do adipocytes provide an appropriate cellular environment for regulated AQP2 trafficking but that this process is distinct from the retention mechanism that facilitates regulated exocytosis of GLUT4. In future studies it will be interesting to determine the endogenous adipocyte membrane and intralumenal cargo proteins that are responsive to increased cAMP levels.

The ability of adipocytes to differentially translocate GLUT4 and AQP2 provided the impetus for investigating the molecular machinery that facilitated the segregation of each protein. In a series of collaborative studies performed with Dr. Giuseppe Procino from the University of Bari, the initial sorting and trafficking behavior of newly-synthesized GLUT4 and AQP2 were directly examined. We first looked at the initial biosynthetic sorting of newly-synthesized transporter by comparing the temporal acquisition of forskolin and insulin-responsiveness of AQP2 and GLUT4, respectively. The data presented recapitulated previous reports (54, 102) showing that newly-synthesized GLUT4 undergoes a time-dependent sorting process that requires 9-12h before displaying full insulin-responsiveness. Surprisingly and in contrast to GLUT4, AQP2 acquired full forskolin-responsiveness within 3 h of biosynthesis. In subsequent studies, we additionally demonstrate that the exit of AQP2 from the TGN was independent of

the adaptor protein GGA, which, in contrast, is needed for sorting of GLUT4 into the insulin-responsive storage compartment. Although the non-dependence on GGA could account for the rapid acquisition of hormone-responsiveness of newly-synthesized AQP2, another possibility is that the protein rapidly defaulted to the plasma membrane and underwent endocytosis into the cAMP-responsive compartment. This scenario, however, is highly unlikely, since we also demonstrated that inhibition of endocytosis by expression of a dominant-interfering dynamin mutant did not affect the ability of newly-synthesized AQP2 to rapidly display cAMP-responsiveness. These data are more consistent with a rapid TGN sorting of AQP2 directly to the cAMP-responsive compartment without having to initially transit the plasma membrane.

Altogether, this study demonstrated the utility of the adipocyte cell system in distinguishing between the trafficking properties of GLUT4 and AQP2. It established the uniqueness of the vasopressin-regulated trafficking of the latter, which can now be considered as fundamentally and operationally different from the insulin-regulated trafficking of GLUT4 in muscle and adipose tissue. Additionally, having indirectly established that the dileucine and phenylalanine-based motifs play non-redundant roles in GLUT4 and AQP2, a more detailed analysis of the functional domains and mechanisms responsible for distinct compartmentalization of each transporter is now possible. Efforts can now be channeled towards identifying the protein and lipid components of each transporter's sorting machinery. Ultimately, this will expand our molecular understanding of the role of the trans-Golgi network in directing distinct trafficking decisions leading to appropriate intracellular compartmentalization.

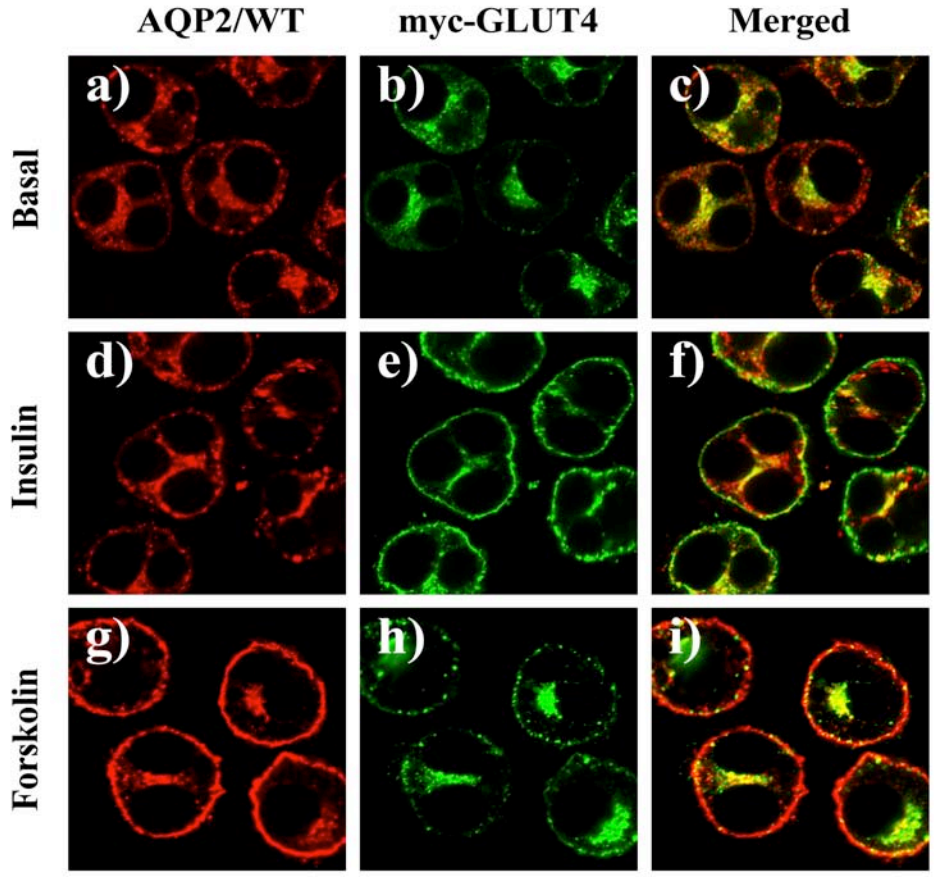

Figure 2.2. Co-expression of myc-GLUT4 and wild-type aquaporin 2 (AQP2/WT) in 3T3-L1 adipocytes. Mature adipocytes were electroporated with 50 μg each of myc-GLUT4 and AQP2/WT cDNA. After 24 h, the cells were either left untreated (a-c) or stimulated with 100 nM insulin (d-f) or 50 μM forskolin (g-i) for 20 mins at 37°C. The specimens were then processed for immunofluorescent microscopy using a monoclonal anti-myc antibody (Sigma) to label GLUT4 and a custom made polyclonal anti-AQP2 antibody to detect WT/AQP2. Each panel is a composite image of representative cells from each condition.

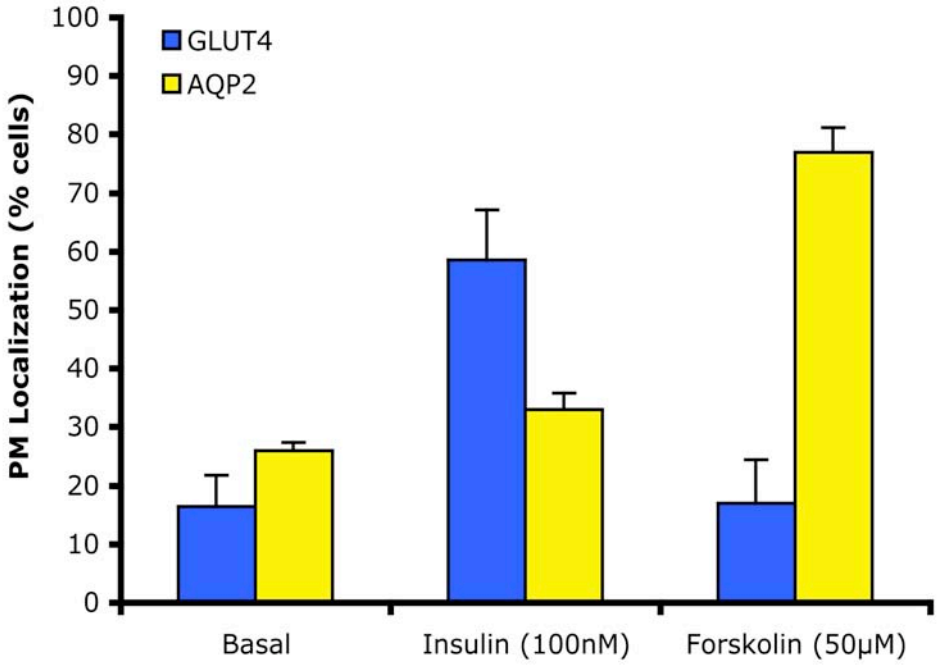

Figure 2.3. Quantification of GLUT4 and AQP2 translocation in response to insulin or forskolin stimulation. The response to insulin or forskolin stimulation was quantified by counting 50 representative cells per condition and taking the fraction of cells displaying a continuous plasma membrane rim. The extent of translocation is expressed as a percentage (means ± SE) of cells with a PM ring as obtained from 3-4 independent experiments.

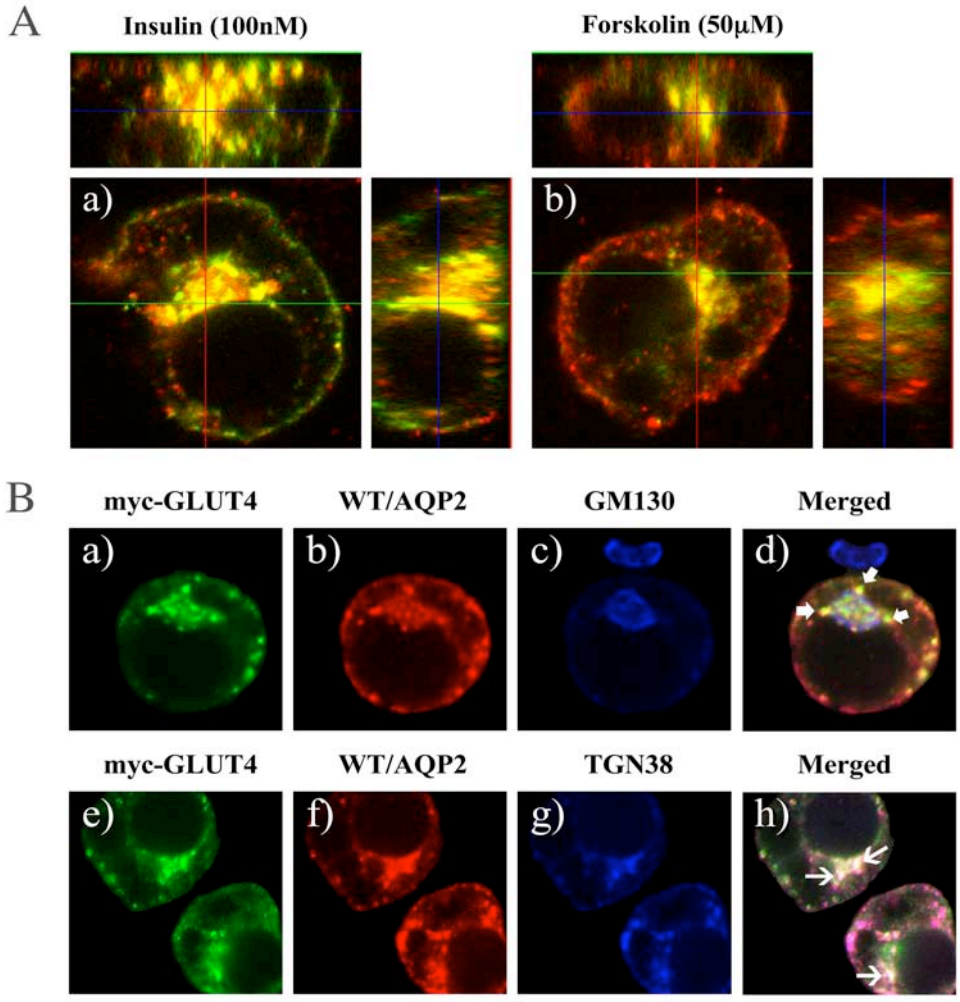

Figure 2.4. Representative images of adipocytes co-expressing myc-GLUT4 and WT/AQP2 showing characteristic localization for each protein. A) XZ and YZ reconstruction of stimulated cells showing partial colocalization within the perinuclear region. B) Co-localization of myc-GLUT4 and WT/AQP2 with the cis-Golgi marker GM130 and the trans-Golgi marker TGN38. Thick arrows (panel d) show non-colocalization with GM130 while thin arrows (panel h) signify colocalization with TGN38.

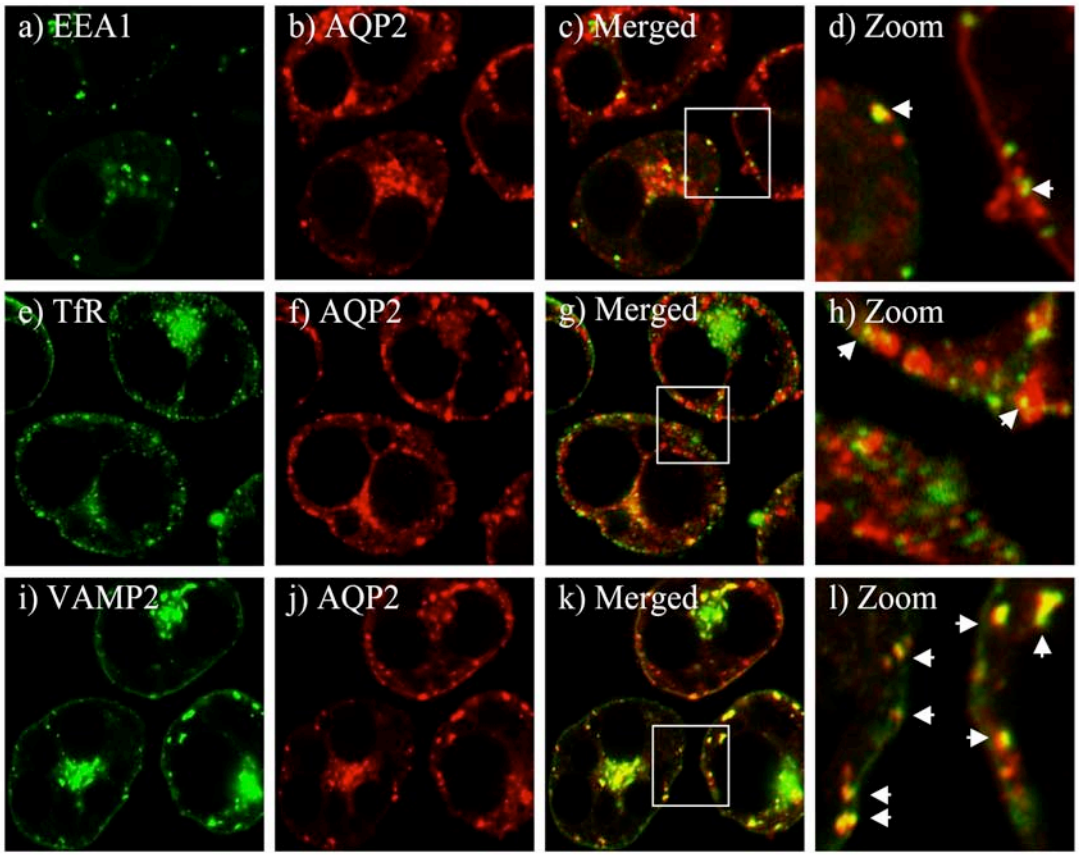

Figure 2.5. Colocalization studies comparing WT/AQP2 compartmentalization with the early endosomal marker EEA1, the human transferrin receptor (TfR) and vesicle-associated membrane protein 2 (VAMP2). Fully differentiated 3T3-L1 adipocytes were cotransfected with 50 μg of AQP2/WT and 50 μg of EEA1-EGFP, human transferrin receptor or VAMP2-EGFP cDNA. 24 hours after transfection, cells were fixed and processed for immunofluorescent microscopy. Representative composite images showing AQP2/WT colocalization with EEA1 (panels a-d), hTfR (panels e-h) and VAMP2 (panels i-l) are shown. Arrows (panels d, h, l) point to overlapping green and red signals, signifying colocalization.

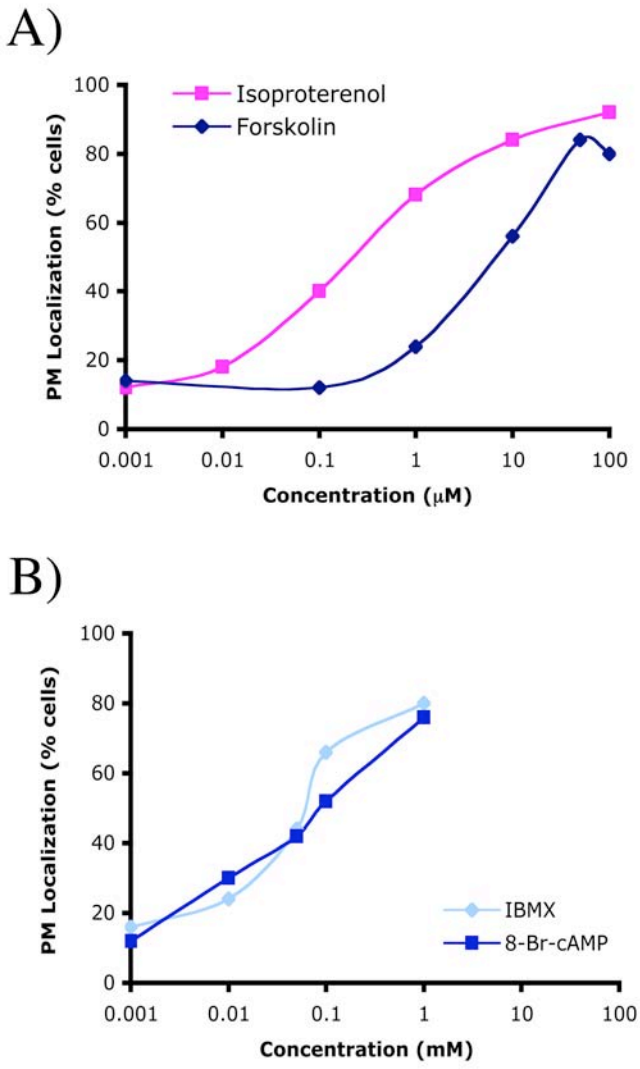

Figure 2.6. Effect of isoproterenol, forskolin, IBMX and 8-bromoadenosine 3'5'-cyclic monophosphate (8-Br-cAMP) on AQP2 translocation. Fully differentiated adipocytes were electroporated with 50 μg of AQP2/WT cDNA. 24 hours after transfection, cells were stimulated with A) isoproterenol (10 nM-100 μM) and Forskolin (100 nM-100 μM) and B) IBMX (1 μM - 1 mM) and 8-Br-cAMP (1 μM- 1mM) for 20 minutes at 37°C. The cells were then fixed, immunolabeled and scored by fluorescent microscopy.

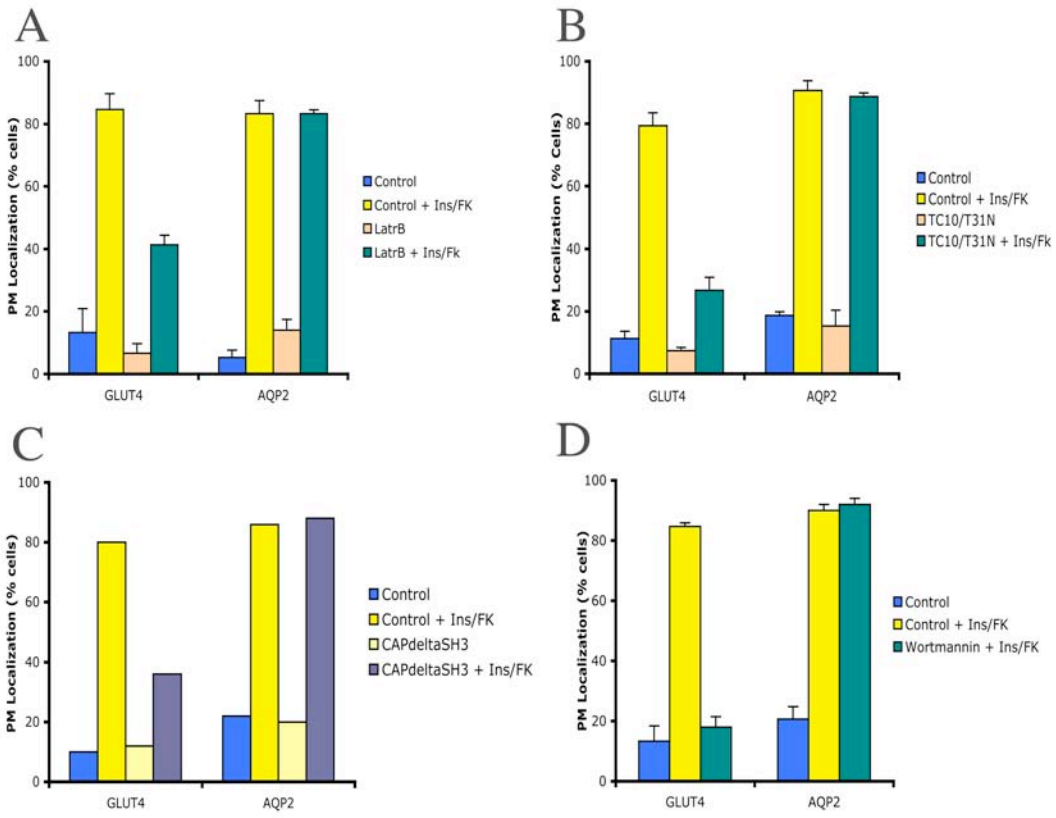

Figure 2.7. Comparison of signaling events that regulate the translocation of GLUT4 and AQP2 in adipocytes. A) Adipocytes overexpressing GLUT4-EGFP or WT/AQP2 were treated with either vehicle or latrunculin B and stimulated with insulin or forskolin. B) Adipocytes were cotransfected with 50 μg of GLUT4-EGFP or WT/AQP2 and 200 μg of TC10/T31N cDNAs. 24 hours after recovery, cells were stimulated with either insulin or forskolin. C) Instead of TC10/T31N, adipocytes were co-transfected with 200 μg CAPΔSH3 cDNA. D) Adipocytes overexpressing GLUT4-EGFP or WT/AQP2 were pretreated with 1 nM wortmannin for 10 minutes before stimulation with insulin or FK. Data presented, except for 2.7C, are average values from 3 independent experiments.

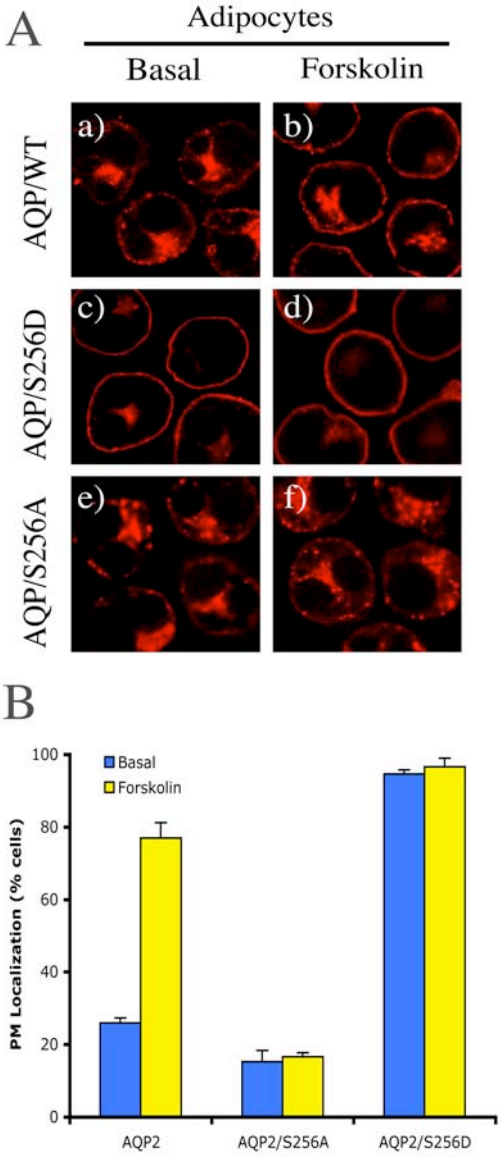

Figure 2.8. Expression of WT/AQP2, AQP2/S256D and AQP2/S256A in adipocytes A) Composite images of representative cells expressing WT/AQP2 (panels a-b), AQP2/S256D (panels c-d) or AQP2/S256A (panels e-f) in basal or forskolin stimulated conditions. B) 50 representative cells per condition were scored based on the presence of a PM rim. The result is expressed as the percentage (means ± SE) of cells showing a PM ring as determined from 3-4 independent experiments.

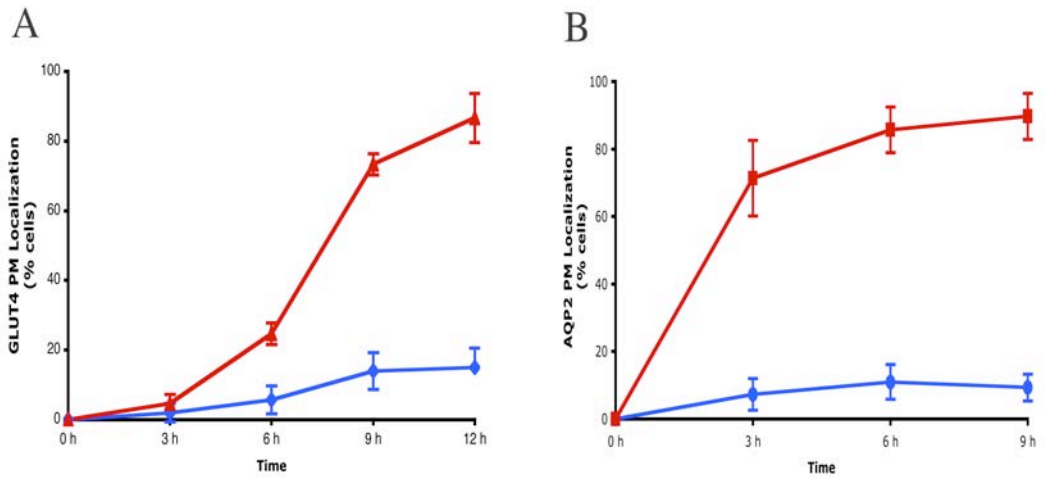

Figure 2.9. Time-dependent acquisition of insulin- and FK-stimulated GLUT4 and AQP2 translocation in adipocytes. A) Mature adipocytes were transfected with 50 µg of GLUT4 cDNA and at the indicated time after electroporation, were incubated with (▲) or without (◆) 100 nM of insulin for 20 minutes. B) Mature adipocytes were transfected with 50 µg of WT/AQP2 cDNA and at the indicated time after electroporation, were incubated with (■) or without (●) 50 µM of FK for 20 minutes. Quantification was done by counting 50 representative cells/condition and computing the fraction of cells showing a PM rim. The data presented is obtained from 3-4 independent experiments. This study was done in collaboration with Dr. Giuseppe Procino from the University of Bari, Italy.

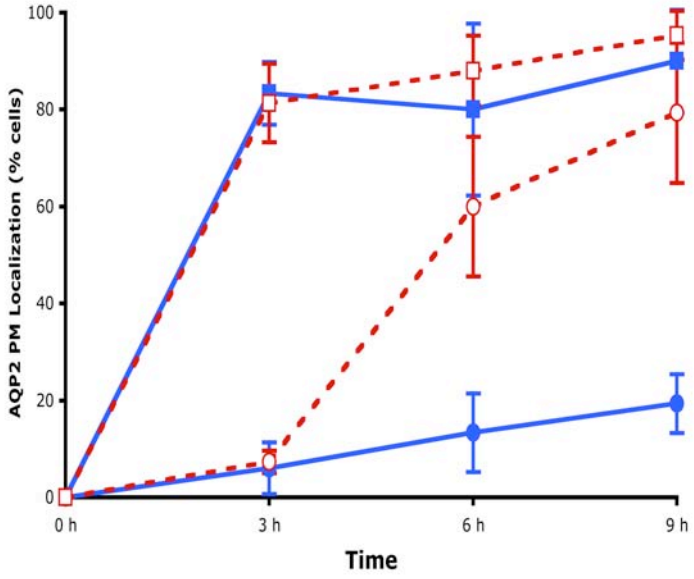

Figure 2.10. Newly-synthesized AQP2 directly gains access to the cAMP-responsive compartment. Fully mature adipocytes were electroporated with 50 μg of cDNA encoding WT/AQP2 plus 100 μg of cDNA encoding GFP-Dyn/WT (solid symbols) or GFP-Dyn/K44A (open symbols). After transfection, cells were treated with Brefeldin A at 5 μg/ml for 3 hours to allow dynamin expression but prevent AQP2 exit from the ER. Cells were thern extensively washed to remove the BFA, and at the time indicated, were incubated with (squares) or without (circles) 50 μM of forskolin for 20 minutes. The cells were then processed for confocal microscopy and each condition was scored as previously described. The study was done in collaboration with Dr. Giuseppe Procino from the University of Bari, Italy.

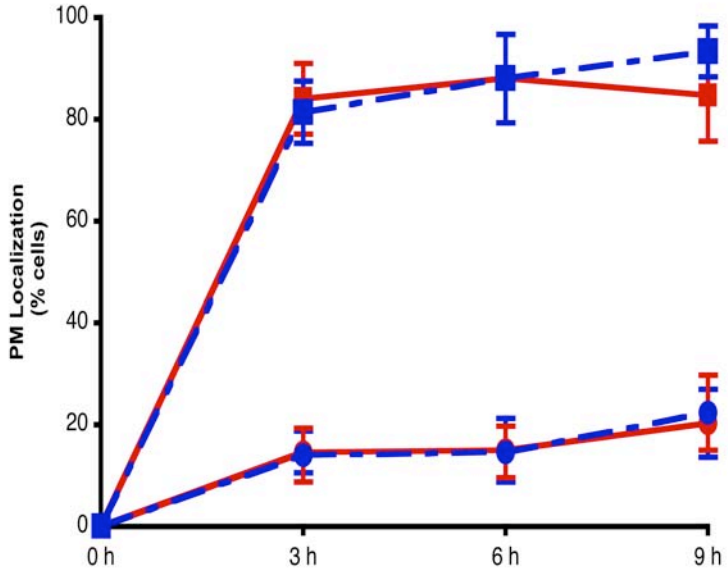

Figure 2.11. Entry of newly-synthesized AQP2 to the cAMP-responsive compartment is not dependent on GGA. Fully mature adipocytes were electroporated with 50 μg of cDNA encoding WT/AQP2 plus 100 μg of cDNA encoding WT/GGA (solid line, red) or dominant-interfering GGA mutant (broken line, blue). After transfection, cells were incubated at the indicated time, with (squares) or without (circles) 50 μM of forskolin for 20 minutes. The cells were then processed for confocal microscopy and each condition was scored as previously described. The study was done in collaboration with Dr. Giuseppe Procino from the University of Bari, Italy.

CHAPTER 3

BIOCHEMICAL AND FUNCTIONAL CHARACTERIZATION OF THE CAVEOLAE-ASSOCIATED PROTEIN AHNAK IN ADIPOCYTES

Insulin is a potent anabolic mammalian hormone essential for the maintenance of normal glucose homeostasis. Binding of insulin to the cell surface insulin receptor in muscle and adipose tissue leads to the phosphorylation of several members of the IRS family of insulin receptor substrate proteins, recruitment and activation of phosphatidylinositol 3-kinase and the formation of phosphatidylinositiol-3,4,5-trisphosphate (PIP3) in the plasma membrane. PIP3 in turn binds to Akt (protein kinase B) which becomes activated via phosphorylation by phosphoinositide-dependent protein kinases 1 and 2. Although the insulin receptor kinase also regulates other signaling pathways necessary for increased glucose transport uptake and GLUT4 translocation, it is well established that Akt activation is fundamentally important based upon studies in tissue culture, animal models and in a naturally occurring human mutation.

Currently, several direct target substrates for the Akt kinase have been identified including those that regulate growth, apoptosis, nutrient sensing and metabolism (63). In the context of GLUT4 trafficking, Akt is suggested to phosphorylate the Rab-GAP protein AS160 on multiple sites to inhibit its Rab GTPase activity (84). Constitutive activation or loss of this Rab GTPase activity results in either an inhibition or stimulation of GLUT4 translocation (62). Other studies have shown that AS160 is not required for the docking/fusion of GLUT4 transport vesicles with the plasma membrane, suggesting that an insulin-dependent activation of Rab activity is necessary for an earlier step in the

translocation process (23). In this regard, a t-SNARE binding protein Synip has also been recently reported to serve as an Akt-dependent substrate necessary for the fusion of GLUT4 transport vesicle in the plasma membrane (75).

This chapter presents the results of a proteomic screen that was undertaken to identify other potential Akt substrates that may be involved in insulin-stimulated GLUT4 translocation in 3T3-L1 adipocytes. In this analysis, AHNAK was identified together with 21 other proteins that carry the Akt phosphorylation motif RXRXXS/T. AHNAK is a 700 kDa protein that was initially identified as a nuclear phosphoprotein whose expression was repressed in a human neuroblastoma cell line. This unusually large protein is a known Akt substrate in epithelial cells and has reported roles in vesicle trafficking, regulation of ion channel conductance and maintenance of epithelial cytoarchitecture. In this study, the expression and intracellular distribution of AHNAK during adipogenesis was characterized and a possible biological function for AHNAK in adipocytes was investigated. To conclude, a model was put together where AHNAK is indirectly involved in the translocation of GLUT4 bearing-vesicles by serving as part of the molecular machinery that keeps cortical actin intact and closely associated with the plasma membrane.

The Lipid Raft-Associated Protein AHNAK

AHNAK, which is Hebrew for "giant," is a 700 kDa protein first identified in 1992 as a gene whose transcription is repressed in a neuroblastoma cell line (86). The protein is rich in apolar and charged residues with a central domain composed of highly conserved repeating elements that are 128 amino acids long. Each repeating element is made up of heptad units that follow the pattern φ±φP±φ±, where φ is a hydrophobic residue, ± is a hydrophilic residue and P is proline. The predicted secondary structure resembles a β-strand with clean

separation of negatively and positively charged residues. The proposed tertiary structure is a 7-8 stranded barrel that forms a polyionic rod 1.2 μm long (86).

In studies done on HeLa cells, AHNAK was shown to be a substrate for Akt phosphorylation *in vitro* and *in vivo* (90). The serine residue located at position 5535 of the C-terminal domain sits within the motif RHRSNSF and is believed to be the putative phosphorylation site for Akt. In this cell line, phosphorylation by Akt is suggested to regulate protein localization, allowing it to translocate from the nucleus to the cytoplasm.

Although the exact cellular function of AHNAK remains unclear, studies done on different cell systems suggest that it may be involved in several processes including ion-channel regulation, vesicle-trafficking and cytoarchitecture remodeling. For instance, studies done on cardiomyocytes reveal that the C-terminal AHNAK domain can effectively sequester the β-subunit of L-type calcium channels to negatively regulate the channel's ion conductance (26). In neuronal cells, AHNAK was reported to be a marker for a specific population of calcium-sensitive vesicles called "enlargeosomes," which are suggested to function in cell membrane differentiation and repair (8, 18). In polarized epithelial cells, AHNAK forms a multimeric complex with actin and the annexin2/S100A complex (6). S100 proteins represent a subgroup of EF-hand calcium-binding proteins and function in cell growth and motility, cell cycle regulation, transcription and differentiation. In this study, the siRNA-mediated ablation of AHNAK expression resulted to stunting of cell growth and flattening of cell morphology suggesting that in this cellular context, the protein is a key regulator of cytoskeletal organization. Recently, the minimal annexin 2 binding motif in AHNAK was mapped to a 20-amino acid peptide stretch in the C-terminal domain (20).

The fact that AHNAK is a reported Akt substrate that has not been studied in the context of insulin signaling provides a compelling impetus for investigating its role in adipocytes. AHNAK's identification in the proteomic screen hints to a possible involvement in GLUT4 trafficking and/or insulin-mediated transcriptional activation. In the next section, the results of studies suggesting that AHNAK is a caveolae-associated structural protein that is essential for cortical actin integrity and insulin-stimulated GLUT4 translocation in adipocytes will be presented.

MATERIALS AND METHODS

Cell Culture and Electroporation

Murine 3T3-L1 pre-adipocyte cell line was purchased from the American Type Tissue Culture (ATCC) repository. Cells were maintained in DMEM supplemented with 25 mM glucose, 10% bovine calf serum and 1% penicillin/streptomycin at 37°C and 8% CO_2. Two days post-confluency, fibroblasts were induced to differentiate into adipocytes by shifting media into DMEM supplemented with 25 mM glucose, 10% fetal bovine serum, 1% penicillin/streptomycin, 1 μg/ml insulin, 0.25 μM dexamethasone and 0.5 mM 3-isobutyl-1-methylxanthine (IBMX). After 4 days, the media was shifted to DMEM with 10% FBS and 1 μg/ml insulin for 4 additional days. Mature adipocytes at 8 to 12 days post-differentiation were used for all studies. In studies requiring transient transfection of cells with siRNA or an expression vector, mature adipocytes were electroporated using the Gene Pulser II (BioRad, Hercules, CA) with settings of 0.16 kV and 960 microfarads. After electroporation, cells were re-plated on collagen coated plates or glass cover slips and allowed to recover in FBS-supplemented medium.

Reagents and antibodies

The polyclonal KIS antibody targeted against a conserved repeating element in the central domain of AHNAK was provided by Dr. Jacques Baudier (22). Antibodies against Akt and phosphorylated Akt (Ser473 and Thr308) were purchased from Cell Signaling Technology (Danvers, MA). The anti-caveolin 1

and 2 and annexin 2 antibodies were obtained from Transduction Laboratories (San Jose, CA). The polyclonal anti-GLUT4 antibody was obtained as previously described (51). The c-myc antibody was obtained from Santa Cruz Biotechnology (Santa Cruz, CA). The anti-rabbit and anti-mouse IgG Alexa-Fluor secondary antibodies were purchased from Molecular Probes, Inc (Carlsbad, CA). The exofacial myc-tagged GLUT4-EGFP/pcDNA3 and GLUT1-EGFP/pcDNA3 were constructed as previously described (50). All other chemicals and reagents used were purchased from Sigma unless otherwise stated.

Western Blotting

For total cell lysates, mature adipocytes were washed twice with ice-cold PBS and collected in lysis buffer (50 mM Tris, pH 8.0, 150 mM NaCl, .05% deoxycholic acid, 1% Triton X-100, 10% glycerol, 2 mM EDTA/EGTA, protease and phosphatase inhibitor cocktails [Sigma]). Lysates were passed through a 26G needle and centrifuged for 10 minutes at 2500 rpm in a standard tabletop centrifuge at 4°C. Supernatant was collected and protein concentration was determined using the BioRad (Hercules, CA) protein assay reagent in a 96-well format. To blot for AHNAK, the lysates were boiled in NuPAGE LDS Sample Buffer mixed with the NuPAGE Sample Reducing Agent and resolved using the NuPAGE 3-8% Tris-Acetate Gel from Invitrogen (Carlsbad, CA). Proteins were blotted onto PVDF membranes using the wet transfer technique at 90 volts for 1.2 h. For experiments looking at other proteins, the lysates were boiled in 1X DTT Laemmli buffer and transferred onto PVDF membranes using the semi-dry technique (BioRad). Membranes were blocked using 1% milk in TBST and immunoblotted using the appropriate antibodies.

Subcellular Fractionation

Adipocyte subcellular membrane fractions were obtained by differential centrifugation. Briefly, mature adipocytes were washed and collected in HES buffer (20 mM HEPES, pH 7.4, 1 mM EDTA, 255 mM sucrose, protease and phosphatase inhibitor cocktails [Sigma]). Cell lysates were prepared by passing the cell suspension through a ball bearing homogenizer from Isobiotec (Heidelberg, Germany). Lysates were then centrifuged at 16,000 x *g* for 20 min at 4 °C. The resulting supernatant was spun at 48,000 x *g* for 20 min at 4 °C to retrieve the low speed pellet (LSP). The supernatant was collected for a second time and centrifuged at 212,000 x *g* for 75 min at 4 °C to generate the high speed pellet and cytosol (supernatant) fractions. The crude plasma membrane pellet obtained after the initial spin was resuspended in HES buffer and layered onto a 1.12 M sucrose cushion and centrifuged at 100,000 x *g* for 70 min to separate the nuclei and mitochondrial debris. The plasma membrane layer was isolated from the sucrose cushion and spun at 48,000 x *g* for 45 min. All pelleted fractions were resuspended in RIPA buffer (150 mM NaCl, 50 mM Tris, 1 mM EDTA, 1% NP-40, 0.5% Na-deoxycholate, 0.1% SDS, pH 7.4) with protease and phosphatase inhibitor cocktails.

Plasma Membrane Sheet Assay

After the appropriate treatments, cells were rinsed once with ice-cold PBS and incubated with 0.5 mg/ml poly-L-lysine in PBS for 30 s. The polycationic nature of this molecule favors interaction with anionic sites on cell cultures and the coverslip surface, thereby acting as an adhesive to minimize loss of membrane sheets. Cells were then rinsed three times in a hypotonic buffer (23 mM KCl, 10 mM HEPES, pH 7.5, 2 mM $MgCl_2$ and 1 mM EGTA) to allow for swelling. Cells were then fixed by incubating in 2% Paraformaldehyde in PBS for 10 minutes.

The enlarged cells were then washed and sonicated for 3 seconds in PBS . The bound plasma membrane sheets were washed twice with PBS and used for indirect immunofluorescence as described below.

RNA Interference

21-nucleotide siRNA duplexes were designed using the target sequence 5'-AAGAUCUCCAUGCCUGAUGUG-3' corresponding to a highly conserved sequence of the repeated domains of AHNAK and purchased from Dharmacon RNA Technologies (Lafayette, CO). The scrambled control sequence used was 5'- CGUCCAUAUACCGGUUCUUUG-3'. For each experiment, 1 nmol of siRNA for every condition was used for transfection. The cells were allowed to recover for 72 hours before further studies were carried out.

Indirect Immunofluorescence and Co-localization Studies

Fully-differentiated adipocytes grown on cover slips were fixed using 4% paraformaldehyde, 0.18% Triton X-100 in PBS for 10 minutes. In the case of plasma membrane sheets, pre-fixing was done before the cells were sonicated. After fixing, the specimens were incubated in blocking buffer (1% BSA, 5% donkey serum in PBS), washed and immunolabeled with the appropriate primary antibodies for 1 h at 37°C. The cover slips were then washed with phosphate buffered saline and labeled with the appropriate Alexa fluorophore-conjugated secondary antibody. After labeling, the cover slips were washed three times and mounted on slides using Vectashield (Burlingame, CA). Specimens were evaluated by visualization on a Zeiss LSM510 confocal fluorescent microscope.

Single-Cell Quantitation

Mature adipocytes transfected with siRNA and myc-GLUT4-GFP or myc-GLUT1-GFP were shifted to serum-starving media (DMEM with 0.1% BSA) on the 55-60th hour post-transfection and allowed to starve for 12-15 hours. After the appropriate treatments (insulin or vehicle), whole cells were fixed using 4% paraformaldehyde in PBS for 10 minutes and labeled using a monoclonal anti-myc antibody (Sta. Cruz). After myc labeling, the cells were washed, permeabilized in 0.18% Triton X-100 for 10 minutes and immunolabeled using the KIS anti-AHNAK antibody. A third round of labeling wash done using the Alexa fluorophore-conjugated antibodies. The specimens were then mounted and evaluated by confocal microcopy. Images of 15 cells per condition were processed using the Zeiss LSM510 software to determine the ratio of plasma membrane myc-signal over the total GFP signal.

RESULTS

AHNAK is enriched in Triton-insoluble fractions obtained from adipocytes.

A crude technique to isolate lipid rafts from mature adipocytes was developed to procure the specimen for proteomic analysis. Cells grown on collagen-coated plates were passively treated with 1% Triton X-100 for 0, 5, 10, 15, 20 and 25 minutes at room temperature. The detergent-insoluble fraction was collected in RIPA buffer and separated by one-dimensional SDS-PAGE. The efficiency of detergent extraction at each time point was determined by immunoblotting for known raft and non-raft proteins (Figure 3.1A). Treatment with Triton for 20-25 minutes efficiently extracted non-raft molecules as reflected by ~90% extraction of transferrin receptor. Additionally, greater extraction of syntaxin 4 was observed compared to SNAP23. This is in agreement with previous work on SNARE proteins in adipocytes which show that SNAP23 more strongly associates with lipid rafts compared to syntaxin 4 (17).

Table 1. Adipocyte lipid raft proteins with RXRXXS/T motif

30 kDa	Prohibitin Ribosomal Protein S3	
44 kDa	Citrate Synthase Sulfide Quinone Reductase-Like	Diacylglycerol-O-Acyltransferase
56 kDa	Aspartyl-tRNA Synthetase Perilipin (KXRXXS)	BCL2-LIKE 3 (RXKXXT)
70 kDa	Lamin A PL10	PCX Protein
80 kDa	Nucleoporin 93 Nucleolin Brain Glycogen Phosphorylase Splicing Factor P/Q Rich	Isopeptidase T Hexokinase II Nucleoporin 107 eTranslation Initiation Factor 3, sub 9
> 160 kDa	Nucleoporin 205 Translocator Promoter Region Protein	AHNAK

To obtain the final specimens for proteomic analysis, cultured adipocytes were stimulated with vehicle or 10 nM of insulin for 20 minutes prior to detergent extraction using 1% Triton X-100 for 25 minutes. For control, whole cell lysates from non-detergent treated, basal and insulin stimulated cells were collected in parallel. All of the fractions were resolved by SDS-PAGE and visualized by silver-staining. Protein bands from the insulin-stimulated, Triton-insoluble lane on the silver-stained gel corresponding to bands on an immunoblot that was ran in parallel and processed using an anti-phosphorylated-Akt antibody were harvested and sent for LC/MS/MS (Figure 3.1B). From the six protein bands that were sent for identification, 21 novel proteins with the Akt-phosphorylation motif RXRXXS/T and 1 known Akt substrate, AHNAK, were identified (Table 1). To confirm that AHNAK is enriched in Triton-insoluble fractions, I retrospectively immunoblotted for AHNAK using the same detergent-insoluble lysates that I obtained while optimizing the protocol for Triton extraction (Figure 3.1A).

AHNAK redistributes to the periphery in association with the plasma membrane and its expression is down-regulated during adipogenesis in 3T3-L1 cells.

22 proteins with the Akt-phosphorylation motif RXRXXS/T (Table 1) were identified in a proteomic analysis of Triton X-100-insoluble membrane fractions obtained from fully differentiated 3T3-L1 adipocytes. AHNAK was selected for further investigation because although the protein has been reported as an Akt substrate in polarized epithelial cells, it has not been studied in the context of insulin signaling and GLUT4 trafficking. Aside from adipocytes, robust AHNAK expression has also been documented in insulin-responsive skeletal muscle cells. It is, thus, plausible that AHNAK, as an Akt substrate, may have a key role in insulin-regulated GLUT4 exocytosis.

The initial study determined the expression profile of AHNAK during differentiation of 3T3-L1 fibroblasts into mature adipocytes. To do this, whole cell lysates were collected from cells at different stages of differentiation and immunoblotted for AHNAK and other differentiation markers (Figure 3.2). It is evident from the Western blot that AHNAK expression is downregulated as fibroblasts differentiate into mature adipocytes. Interestingly, annexin 2, which is reported to form a complex with AHNAK in polarized epithelial cells, exhibited a similar profile. Caveolin-1 and GLUT4 were used as markers for positive upregulation. Using whole cell immunofluorescence, the intracellular localization of AHNAK was investigated to determine whether the change in level of expression during differentiation is associated with redistribution of the protein (Figure 3.3). In MDCK cells, AHNAK redistributes from the cytoplasm to a cortical localization as cell density increases and cell to cell contacts are established (6). Since fibroblasts are too flat to allow for conclusive evaluation of protein localization, fibroblast monolayers were briefly treated with 0.25% trypsin to incompletely release the cells from attachment to the cover slip. In undifferentiated fibroblasts, AHNAK is excluded from the nucleus and is mostly scattered in the cytoplasm (Figure 3.3, panels a-b). In contrast, AHNAK in mature adipocytes exhibits a primarily peripheral localization and closely associates with the plasma membrane (Figure 3.3, panel c). Higher magnification images further revealed that AHNAK in fully-differentiated adipocytes is not homogenously juxtaposed to the plasma membrane but is positioned in punctate clusters adjacent to the plasma membrane (Figure 3.3, panel d). Since the predicted structure of the protein shows no transmembrane domains and it was initially observed that in non-permeabilized cells, AHNAK is inaccessible to immunolabeling (data not shown), the intracellular localization of AHNAK was further investigated by subcellular fractionation and immunoblotting. Surprisingly, AHNAK partitioned mostly with the membrane-bound vesicular fraction represented by the high-speed

and low-speed pellets (Figure 3.4). A very small fraction was identified in the cytoplasm and no detectable level was seen in either the plasma membrane or the nuclear/mitochondrial fraction. Actin was used to label the cytoplasm and caveolin-1 was used to mark the plasma membrane. The re-distribution of AHNAK to the periphery during adipogenesis and its and its clear partitioning with vesicles during fractionation suggest that the protein has an intrinsic affinity to lipidogenous membranes. Additionally, this could indicate that AHNAK is particularly involved in vesicular trafficking and in the regulation of cytoarchitecture in fully differentiated adipocytes.

AHNAK associates with caveolin-enriched microdomains in the plasma membrane.

The original objective for the proteomic analysis of Triton X-100 insoluble membrane fractions from adipocytes was to identify lipid raft associated proteins that may be involved in insulin signaling and/or GLUT4 trafficking. Since lipid rafts were operationally defined in this study as nonionic detergent-insoluble and caveolin-enriched membrane fractions, I investigated the possibility that AHNAK is naturally associated with caveolar structures in fully differentiated adipocytes. In separate flotation studies done on MDCK and rat pheochromocytoma (PC12) cell line, AHNAK has been shown to partition almost exclusively with caveolin-1 (6, 18). To test whether AHNAK will exhibit the same property in adipocytes, I prepared plasma membrane sheets from mature adipocytes and co-labeled with AHNAK and caveolin-2 (Figure 3.5). In adipocytes, caveolae are known to organize into structured clusters that are readily identifiable by confocal microscopy. High-resolution images taken from plasma membrane sheets pre-fixed with 2% paraformaldehyde reveal a strong and unmistakable co-localization of AHNAK with caveolin-2 (Figure 3.5, panel c).

Although the fluorescent signal from each protein were more vivid at slightly different planes, suggesting that the overlap may be a result of stacking, both proteins formed the elegant rosette structures characteristic of adipocyte caveolae. Since AHNAK precipitates with membrane-bound vesicles during fractionation, it seemed counter-intuitive that the protein will remain associated with caveolae during the preparation of plasma-membrane sheets. The strong association of AHNAK with caveolae could have resulted, in part, from pre-fixing cells with paraformaldehyde prior to sonication (see methods) during the preparation of the membrane sheets. To test this, the co-localization of AHNAK and caveolin-2 was examined in PM sheets prepared without pre-fixing (Figure 3.5, panels d-f). As expected, AHNAK association with caveolae was significantly reduced in membrane sheets prepared from cells sonicated soon after swelling. Looking at the fluorescent signal from immunolabeled AHNAK, however, the outline of rosette structures are still discernible, suggesting that AHNAK's association with the cytoplasmic leaflet of the plasma membrane is primarily facilitated by caveolar structures. To reconcile these with the results of the cellular fractionation study, it is quite possible that AHNAK segregated with the vesicular fraction because it has a stronger affinity to caveolae found in vesicular membranes. Alternatively, AHNAK's association with the PM could have been disrupted with the mechanical shearing required to break the cells apart and, by virtue of its size, AHNAK could have precipitated with the vesicular pellets during the sequential centrifugation, instead of staying soluble in the cytoplasm. In any case, the results suggest that AHNAK is a peripheral membrane protein that interacts with the plasma membrane with low affinity.

AHNAK association with the plasma membrane is cholesterol-dependent.

Caveolin is a cholesterol-binding protein that can induce and is required for the formation of plasma membrane caveolae. Reversible disruption and flattening of these microdomains can be achieved by incubating intact cells with cholesterol-chelating agents. To investigate the extent by which AHNAK's association with the plasma membrane is dependent on the presence of intact caveolae, the effect of cholesterol depletion and caveolar disruption on the intracellular distribution of AHNAK was further investigated. In polarized canine epithelial cells, cholesterol sequestration abrogated the observed clustering of AHNAK at sites of cell to cell contacts (6). A similar effect is likely to be observed in adipocytes, where AHNAK clustering was documented at membrane caveolar pits. To extract plasma membrane cholesterol from mature adipocytes, cells were incubated in 10 mM methyl-β-cyclodextrin at 37°C for 30 minutes prior to pre-fixing and preparation of plasma membrane sheets (Figure 3.6) or processing for whole cell immunofluorescence (Figure 3.7). In PM sheets prepared from cholesterol-depleted cells, total disruption of highly ordered caveolar structures was apparent (Figure 3.6, panel d). In addition, the membrane preparations also lost any detectable presence of membrane-associated AHNAK (Figure 3.6, panel e). Similarly, representative images taken from intact cholesterol-depleted cells show complete interruption of cortical layering and marked intracellular redistribution of AHNAK (Figure 3.7, panels c-d). Together, these data indicate that the association of AHNAK with the plasma membrane in mature adipocytes is dependent, for the most part, on the presence of cholesterol and intact caveolae. However, the possibility that the peripheral partitioning of AHNAK is facilitated by another caveolar resident protein has not been totally ruled out.

Down-regulation of AHNAK expression interferes with cortical actin organization.

The role of AHNAK as a structural molecule is suggested by studies showing a direct interaction between the protein and the actin-based cytoskeleton. In cardiomyocytes, the carboxy-terminal region of AHNAK binds G-actin and cosediments with F-actin (26). In MDCK cells, AHNAK forms a multimeric complex with actin and annexin 2 and has been implicated in the regulation of the cytoskeleton as epithelial cells polarize and gain height (6). Since actin is also known to reorganize during differentiation of 3T3-L1 fibroblasts into mature adipocytes, AHNAK could be playing a similar role in adipocytes by facilitating cortical stratification of actin in fully-differentiated adipocytes. To test whether the association of AHNAK with the cytoplasmic leaflet of the plasma membrane is dependent on the presence of an intact cortical actin belt, the association of AHNAK with caveolar pits on plasma membrane sheets prepared from cells pre-treated with or without latrunculin B was compared. (Figure 3.8) Latrunculin B is an actin monomer sequestering agent that disrupts the formation of an actin-based scaffold (Figure 3.8, panels a and e). In PM sheets prepared from cell pre-treated with latrunculin B, the association of AHNAK with the plasma membrane is not affected (Figure 3.8, panels f-h). Both AHNAK and caveolin-2 are maintained in the characteristic rosette formation suggesting that the caveolae-mediated association of AHNAK with the plasma membrane is not dependent on the presence of an intact cortical actin scaffold. Representative confocal images taken from intact cells pre-treated with or without latrunculin B and immunolabeled for AHNAK confirm that disruption of cortical actin has no effect on the intracellular localization of the protein (Figure 3.9). We then investigated whether AHNAK plays a role in the maintenance of the cortical actin belt by abrogating the expression of the protein using small-interfering RNA oligonucleotides targeted

against a highly-conserved sequence in the central repeating domain of AHNAK. The technique effectively and specifically depleted AHNAK levels in mature adipocytes as reflected by a representative Western blot looking at AHNAK, annexin 2 and a TGN-resident protein p115 (Figure 3.10A). By confocal microscopy, the efficient downregulation of AHNAK expression was also apparent, with cells showing very little or almost no detectable labeling of AHNAK (Figure 3.10B, panels a and d). Concomitant labeling of actin was done using rhodamine-conjugated phalloidin to observe the effect of AHNAK downregulation on cortical actin organization. In cells where expression of AHNAK was almost totally abrogated (Figure 3.10B, panel d), the effect on cortical actin was strikingly marked, with actin redistributing to the cytoplasm and the cortical belt appearing indistinct and nebulous and almost completely disrupted (Figure 4D, panel e). In cells where AHNAK was not as efficiently depleted and immunolabeling shows residual expression of the protein (Figure 3.10B, panel d, arrowheads), the effect on cortical actin was more subtle. The cells, in this condition, may show some blurring of the actin-based scaffold or, in most cases, will exhibit uneven layering of cortical actin (Figure 3.10B, panel e, arrowheads). A distinct structure called Cav-actin has been described in adipocytes to signify the unique association of actin with caveolar rosettes in this cell system (49). Since AHNAK depletion profoundly affects the formation of cortical actin, it is quite possible that cav-actin structures are also altered when AHNAK expression is inhibited. To test this, cells transfected with scramble or AHNAK-specific siRNA and triple-labeled for caveolin-2, actin and AHNAK were evaluated for the presence of cav-actin (Figure 3.11). As expected, in cells where AHNAK is efficiently depleted, the formation of cav-actin structure was significantly reduced. Although residual actin can still be detected within caveolar rosettes (Figure 3.11, panel f), it is markedly diminished compared to AHNAK-

expressing cells. Altogether, data from these studies suggest that AHNAK plays a structural role in adipocytes by keeping the cortical actin intact.

AHNAK is essential for insulin-regulated GLUT4 translocation.

Current models of membrane trafficking events generally recognize an important role for the cytoskeleton in facilitating the movement of cargo-loaded vesicles to and from the plasma membrane. In the case of GLUT4, several lines of evidence suggest that insulin-stimulated actin remodeling is a key requirement for the effective mobilization and PM translocation of GLUT4-bearing vesicles. Early studies examining the role of actin in insulin signaling demonstrated that depolymerization of cortical actin can effectively inhibit insulin-induced glucose uptake and GLUT4 translocation. Additionally, treatment with actin sequestering agents have been shown to adversely affect the integrity of the GLUT4 storage compartment. In the PI3K-independent pathway of insulin signaling that leads to GLUT4 translocation, the downstream effector TC10 is a well-recognized regulator of actin organization and it is thought that the insulin-induced dynamic actin rearrangement needed for GLUT4 translocation is partly facilitated by the caveolae-restricted TC10. AHNAK, by virtue of its role in maintaining the integrity of cortical actin, could be indirectly involved in the translocation of GLUT4-containing vesicles to the plasma membrane in response to insulin. In studies done on epithelial cells, AHNAK has been characterized as an Akt substrate, both in vitro and in vivo (95). To examine whether AHNAK has any role in insulin signaling that leads to Akt activation, insulin-stimulated Akt activation in cells depleted of AHNAK was evaluated. (Figure 3.12). The results of the study showed no significant differences in Akt activation, as suggested by equivalent phosphorylation of Akt at serine 273 and threonine 308 in response to insulin stimulation, between control and siRNA-treated cells. This suggests that

the role of AHNAK on GLUT4 translocation, if any, is implemented downstream of Akt.

The effect of reduction in AHNAK expression on GLUT4 translocation was then evaluated by confocal microscopy. Fully differentiated adipocytes were co-transfected with myc-GLUT4-GFP and either scrambled siRNA or AHNAK-specific siRNA. As a separate control to evaluate the specificity of any effect for GLUT4, a parallel study was done in cells co-transfected with myc-GLUT1-GFP. 72 hours after electroporation, the cells were serum-starved, stimulated with vehicle or insulin, and processed for microscopy. For every condition, the fraction of the total cell population that was able to mobilize GLUT4 in response to insulin stimulation was evaluated by randomly selecting 50 cells per condition and scoring for the presence or absence of a green fluorescent plasma membrane rim. This PM rim represents signal emanating from GFP and signifies GLUT4 that is localized to the plasma membrane. In conditions where AHNAK was depleted, an average of approximately 45% of cells were able to induce translocation of GLUT4 in response to insulin (Figure 3.13). As expected, myc-GLUT1-GFP defaulted to the plasma membrane and AHNAK depletion and insulin stimulation did not have any significant effect on its localization.

To test the possibility that some cells were still able to translocate GLUT4 after AHNAK depletion because of the varying efficiency of AHNAK knockdown between cells, adipocytes were individually evaluated for their capacity to mobilize GLUT4 in response to insulin. Briefly, cells overexpressing myc-GLUT4-GFP were fixed and labeled using an anti-myc antibody shortly after stimulation with vehicle or insulin. The myc epitope in GLUT4 was cloned in the first exofacial loop of the transporter and will only be accessible for labeling when GLUT4 is situated at the plasma membrane. After myc-labeling, the cells were permeabilized, labeled with anti-AHNAK antibody and processed for immunofluorescent microscopy. For every cell selected for quantitation, the

myc/GFP ratio was computed, where myc is a measure of the fluorescent signal from GLUT4 located on the plasma membrane, and GFP is a measure of total GLUT4 population in a cell. As in the previous experiment, a parallel study was done in cells overexpressing myc-GLUT1-GFP. For control cells electroporated with scrambled siRNA, 15 cells were randomly selected for single-cell quantitation. In the case of AHNAK-depleted cells, 15 adipocytes with ~90% depletion of AHNAK were selected for quantitation. Insulin stimulation resulted to a 20 fold increase in membrane localized GLUT4 in control cells transfected with scrambled siRNA (Figure 3.14). In contrast, GLUT4 translocation in response to insulin stimulation was totally impaired in cells where AHNAK is efficiently depleted. As expected, GLUT1 defaulted to the plasma membrane and insulin stimulation and AHNAK depletion did not show any significant effect. Evidently, the effect of AHNAK depletion on GLUT4 translocation will manifest only after a certain threshold of downregulation is reached. Take together, the results of these studies suggest that AHNAK in adipocytes is an essential component of the molecular machinery that facilitates insulin-stimulated GLUT4 exocytosis.

DISCUSSION

One aspect of the expanding role of caveolae in insulin signaling and GLUT4 trafficking in adipocytes is their involvement in the regulation of the actin-based cytoskeleton. During adipocyte differentiation, the development of highly structured caveolae occurs concomitantly with the formation of a cortical actin lining adjacent to the plasma membrane (45). In fully-differentiated adipocytes, a unique F-actin structure called cav-actin has been documented to enucleate from organized caveolar rosettes (48). While the biological significance of cav-actin remains unclear, it provides a morphological link to suggest that caveolar microdomains are important for dynamic actin reorganizaton. Recently, a more concrete connection between caveolae and actin regulation was established when the functionality of TC10, a potent actin regulator, was found to be dependent on its compartmentalization within caveolar microdomains (104).

In this study, AHNAK was introduced as a caveolae-associated structural protein in adipocytes that is essential for cortical actin stability and translocation of GLUT4. Studies done on polarized epithelial cells characterized AHNAK as a cytosolic protein associated with the inner leaflet of the plasma membrane (6). In MDCK cells, AHNAK redistributes from the cytosol to the plasma membrane at sites of cell-cell contacts before spreading all over the plasma membrane (6, 91). AHNAK undergoes a similar redistribution pattern as fibroblasts differentiate into mature adipocytes. Additionally, AHNAK's expression is negatively regulated during adipogenesis. These findings may be interpreted as indications for a more specialized function for AHNAK in terminally differentiated adipocytes. AHNAK's redistribution to the plasma membrane is comparable to the

dramatic reorganization of stress fiber type F-actin in preadipocytes to cortical F-actin in mature adipocytes. When taken in consideration of the fact that in other cell systems, AHNAK and actin have been shown to physically interact, it seems reasonable to speculate that AHNAK is part of the molecular machinery that supports the characteristic cytoarchitecture of the mature adipocyte (50).

The precipitation of AHNAK with membrane-bound vesicles during subcellular fractionation was unexpected and suggests that AHNAK has a biochemical propensity to interact with lipidogenous membranes. This data agrees with the results of fractionation studies done using the PC12 pheochromocytoma cell line. Borgonovo et al illustrated that in neuroendocrine cells, AHNAK is a specific marker for a unique population of vesicles called enlargeosomes that may be involved in cell differentiation and membrane repair (8). In adipocytes, however, the association of AHNAK with the vesicular fraction could just be a reflection of its lipophilic nature. The proposed structure of the protein depicting a polyionic rod 1.2 μm long is compatible with the results of our immunofluorescent studies showing punctate collections of AHNAK approximately 1 μm in diameter clustered beneath the plasma membrane. Shtivelman et al. suggested that because of the polyionic nature of the protein, molecules of AHNAK may form aggregates to share a restricted space. A more compelling point, however, is the fact that the size of vesicles, which are in the order of 50-100 nm, precludes them from being adequately resolved by light microscopy. Although it is possible that the well resolved AHNAK signal observed are clusters of vesicles docked on the plasma membrane, based on what is known regarding the intracellular distribution of various endosomal markers and the insulin-responsive GLUT4 compartment in adipocytes, it is difficult envision any known vesicular protein that may have this illustrated type of distribution.

The strong association with caveolar rosettes that was observed on plasma membrane preparations and the peripheral localization that was apparent on whole cell immunofluorescent studies confirm that AHNAK in adipocytes is a peripheral membrane protein naturally associated with the plasma membrane. The data also suggests that AHNAK's cortical localization is primary facilitated by direct or indirect interaction with intact caveolae or a resident caveolar protein. When PM sheets were prepared without pre-fixing, the preparations lost most of the associated AHNAK. Similarly, when caveolae were disrupted by depleting membrane cholesterol, the plasma membrane association was lost and AHNAK redistributed intracellularly. These results complement published data on MDCK and PC12 cells showing that AHNAK co-fractionates with caveolin in membrane flotation gradient studies (6, 18). Cholesterol depletion in these cells also resulted to peripheral dissociation of AHNAK suggesting that the cholesterol dependence of its membrane association is universal.

Several groups have suggested that AHNAK is a structural protein that functions in conjunction with actin to support cellular architecture. Depletion of AHNAK in adipocytes did not result in any obvious morphological phenotype but did alter the organization of cortical actin. Previously, our group described a unique association between caveolae and actin in adipocytes and suggested a role for caveolar structures in the formation of F-actin in the plasma membrane (48). The results the current studies suggest the AHNAK may be the anchor that links F-actin to membrane caveolae. The reduction in AHNAK expression induced by siRNA may have interrupted the "molecular glue" that stabilized cortical actin and held it in apposition with the plasma membrane. Along the same line, the inhibitory effect of AHNAK depletion on GLUT4 translocation could be a consequence of cortical actin destabilization. Insulin-induced remodeling of the actin-based cytoskeleton is generally recognized as an essential prerequisite to GLUT4 translocation. AHNAK, by keeping cortical actin in the right position, is

most likely indirectly involved in GLUT4 exocytosis. The membrane localization of AHNAK in MDCK cells is facilitated by direct physical interaction with the actin-associated protein annexin 2 (6). Recently, Huang et al described annexin 2 as a thiazolidinedione-responsive gene essential for GLUT4 translocation (29). Although the authors did not speculate on a possible mechanism, the current study raises the possibility that annexin 2 forms a complex with AHNAK in adipocytes to buttress cortical actin to the plasma membrane.

In conclusion, the results of the studies presented support a model where AHNAK in adipocytes is a molecular bolt that anchors the cortical actin scaffold to the plasma membrane at sites of caveolar formations. The inherent affinity of AHNAK to vesicular membranes may indicate that AHNAK also has a role in vesicle trafficking, particularly at adapting docked vesicle to the cytoskeleton and to sites of membrane fusion. However, the present study suggests the AHNAK's involvement in GLUT4 trafficking is indirect and likely mediated through its role in stabilizing cortical actin. Additionally, the fact that AHNAK has been characterized as an Akt substrate opens the possibility that the reported insulin-induced dynamic reorganization of cortical actin is facilitated via direct regulation of AHNAK.

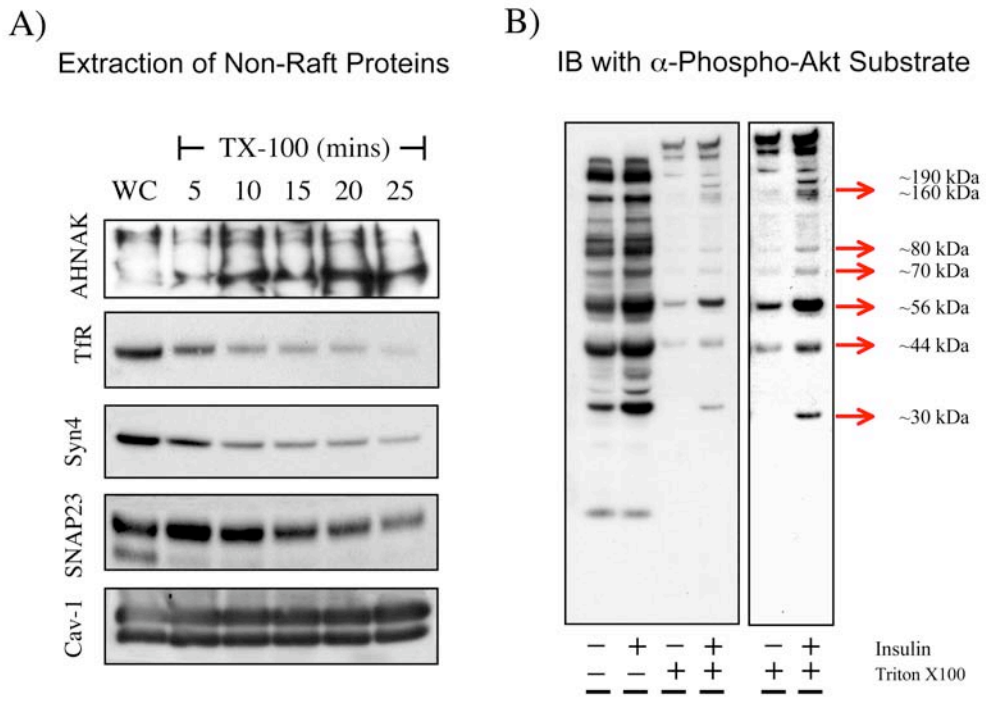

Figure 3.1. Collection of adipocyte lipid raft fractions for proteomic analysis. A) Mature adipocytes were incubated in 1% Triton X-100 in PBS for 0, 5, 10, 15, 20 and 25 minutes. The Triton insoluble fraction was collected in RIPA buffer and 10 μg of total protein per condition was resolved by SDS-PAGE and immunoblotted for transferrin receptor (TfR), syntaxin 4 (Syn4), SNAP23 and caveolin-1 (Cav-1). B) Adipocytes in basal and insulin stimulated conditions were incubated in vehicle or 1% Triton X-100 for 25 minutes at room temperature. The specimens were then collected in RIPA buffer and 10 μg of total protein were resolved by SDS-PAGE and immunoblotted using a phosphorylated-Akt substrate antibody. Contrast was adjusted for the last two lanes to highlight the bands which were picked for identification. The bands on a separate silver-stained gel corresponding to the bands on the immunoblot were harvested and sent for LC/MS/MS.

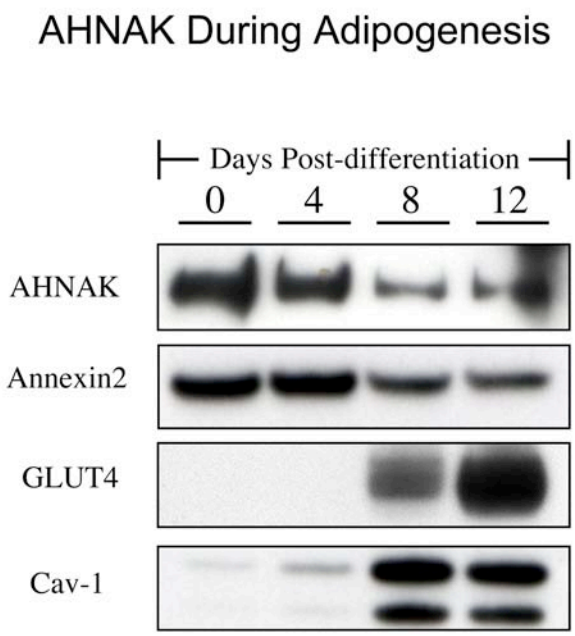

Figure 3.2. AHNAK is downregulated during adipogenesis. Whole cell lysates were collected from cells at 0, 4, 8 and 12 days after differentiation. 30 μg of total protein per condition were resolved by SDS-PAGE and immunoblotted for AHNAK and annexin 2. GLUT4 and caveolin-1 were used as markers for upregulation.

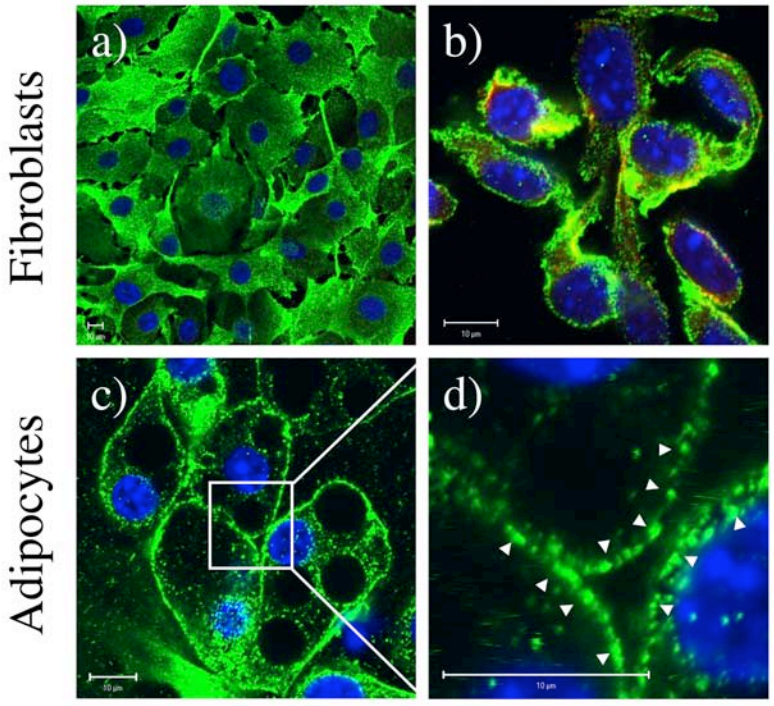

Figure 3.3. AHNAK redistributes as fibroblasts differentiate into mature adipocytes. Fibroblasts were either directly fixed in 2% paraformaldehyde (panel a) or pre-treated with 0.25% Trypsin for 20 seconds prior to fixation (panel b), immunolabeled for AHNAK (green) and processed for fluorescent microscopy. DAPI was used to label the nucleus. Mature adipocytes at 12 days after initiation of differentiation were similarly processed after direct fixation (panels c and d). Arrowheads point to clusters of AHNAK in adipocytes that are apposed to the plasma membrane. The scale bar is equivalent to 10 μm.

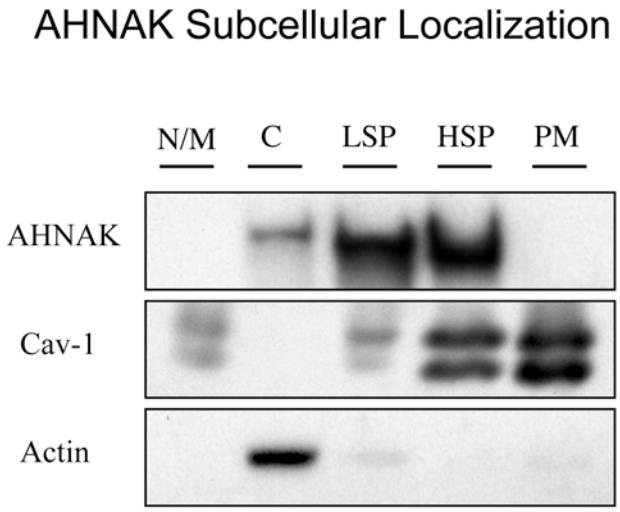

Figure 3.4. AHNAK partitions with the particulate fraction during differential centrifugation. Mature adipocytes at 8-12 days post-differentiation were collected for differential centrifugation to separate the nuclear/mitochondrial (N/M), cytoplasmic (C), low-speed pellet (LSP), high-speed pellet (HSP) and plasma membrane (PM) fractions. 30 μg of protein from each fraction were resolved by SDS-PAGE and immunoblotted for AHNAK, caveolin-1 and actin.

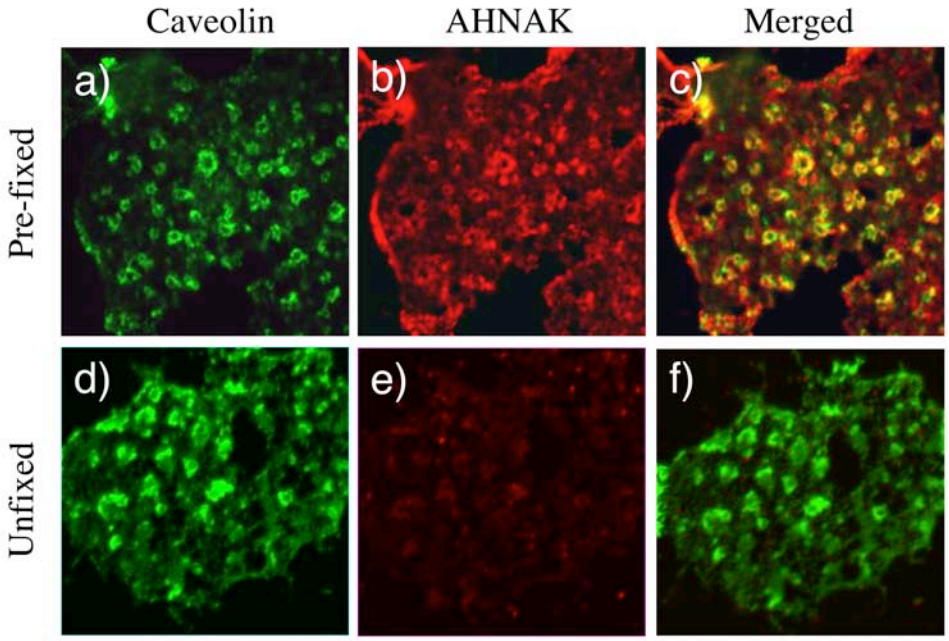

Figure 3.5. AHNAK associates with caveolae in mature adipocytes. Plasma membrane sheets were prepared from fully mature adipocytes that were pre-treated with (panels a-c) or without (panels d-f) 2% paraformaldehyde in PBS for 10 minutes prior to sonication. The membrane preparations were immunolabeled and processed for fluorescent confocal microscopy to compare the localization of caveolin-2 (panels a and d) and AHNAK (panels b and e). These are representative images from three independent experiments.

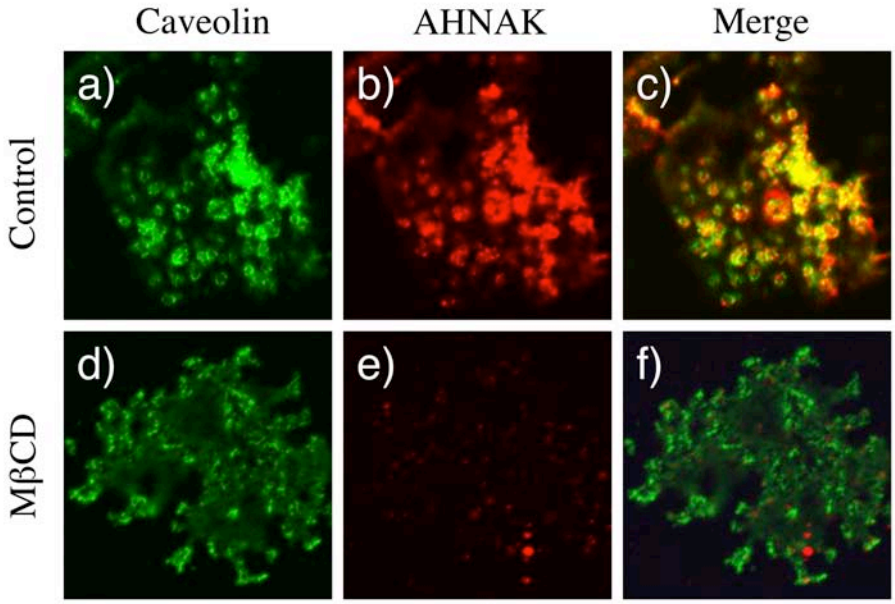

Figure 3.6. Cholesterol depletion disrupts the association of AHNAK with the plasma membrane. Mature adipocytes were treated with or without 10 mM methyl-β-cyclodextrin for 30 min to deplete membrane cholesterol. After MβCD treatment, plasma membrane sheets were prepared and processed for confocal microscopy. Immunolabeling was done using anti-caveolin-2 (panels a and d) and anti-AHNAK antibodies (panel b and e).

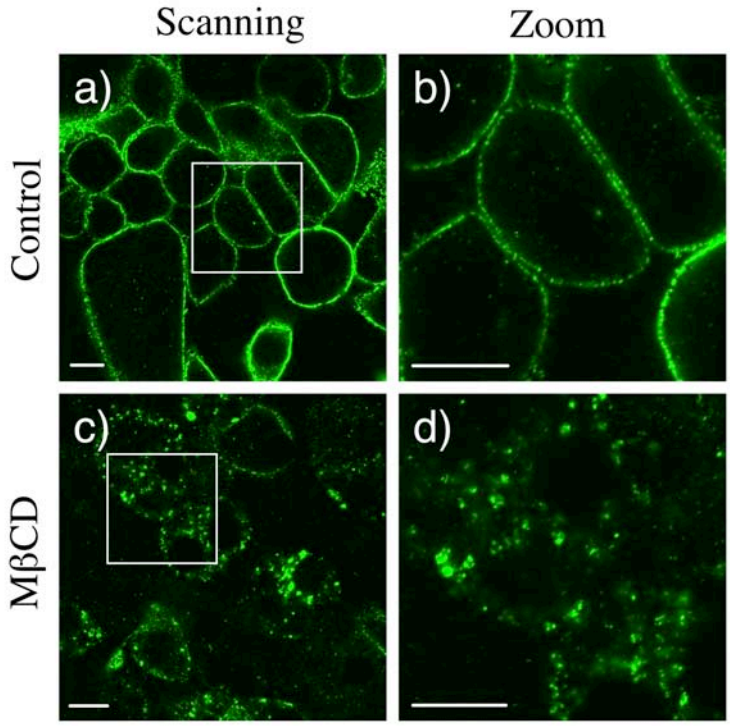

Figure 3.7. Cholesterol depletion induces intracellular redistribution of AHNAK. Whole cells treated with (panels c and d) or without MβCD (panels a and b) were fixed, permeabilized, labeled with anti-AHNAK antibody and subjected to confocal microscopy. The images presented are representative of three independently performed experiments. The scale bar is equivalent to 10 μm in length.

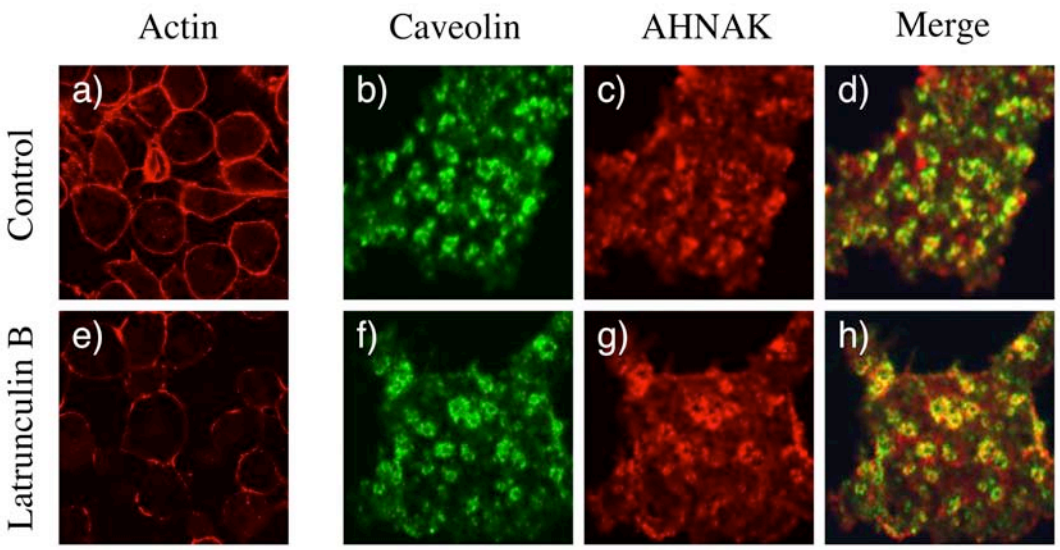

Figure 3.8. Association of AHNAK with caveolae is independent of cortical actin. Plasma membrane sheets were prepared from mature adipocytes treated with or without 20 μM of latrunculin B for 120 minutes to disrupt cortical actin. A separate preparation of whole cells was labeled in parallel using rhodamine-phalloidin (panels a and e) to ascertain disruption of the actin-based cytoskeleton. The membrane preparations were immunolabeled using anti-caveolin-2 (panels b and f) and anti-AHNAK (panels c and g) antibodies.

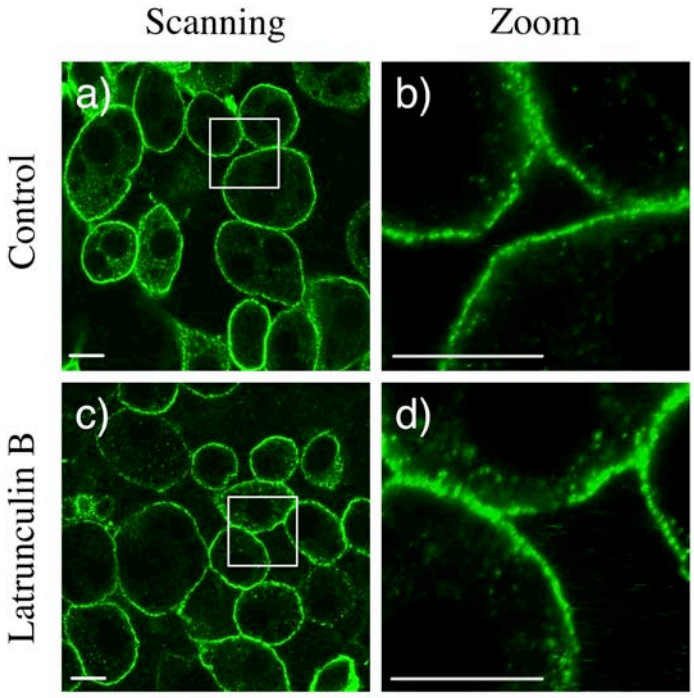

Figure 3.9. Disruption of cortical actin does not affect the association of AHNAK with the plasma membrane. Whole cells treated with or without latrunculin B were fixed, labeled using anti-AHNAK antibody and processed for confocal microscopy. The scale bar presented is equal to 10 μm.

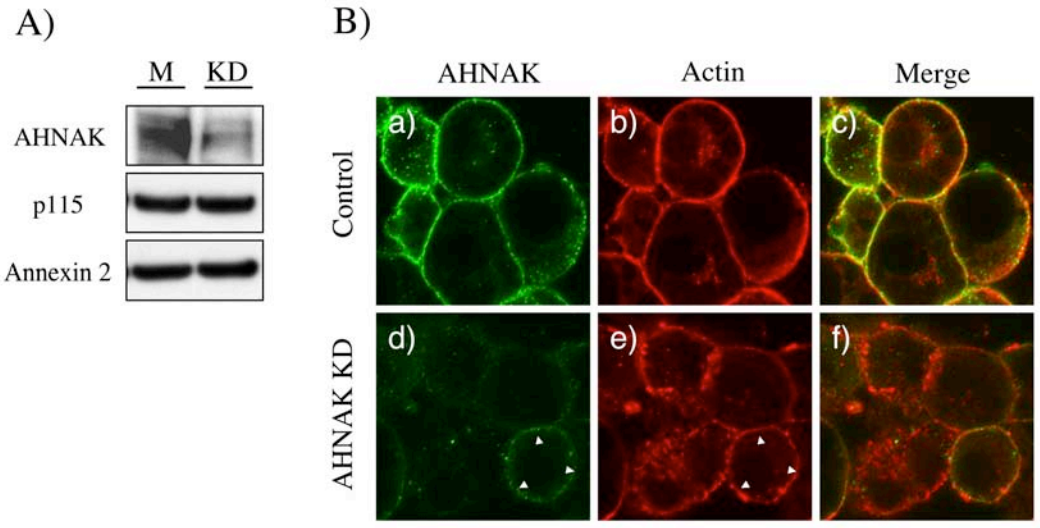

Figure 3.10. AHNAK depletion causes disruption of cortical actin. A) Fully differentiated adipocytes were transfected with 2 nM of either random siRNA (C-control) or AHNAK-specific siRNA (KD-knockdown). 72 hours after, whole cell lysates were collected and 30 μg of total protein were resolved by SDS-PAGE and immunoblotted for AHNAK, p115 and annexin 2. B) Fully differentiated adipocytes transfected with either random (panels a-c) or AHNAK-specific siRNA (panels d-f) were fixed, permeabilized and labeled using anti-AHNAK antibody (panels a and d) and rhodamine-phalloidin (panels b and e). Arrowheads indicate the outline of a cell with incomplete depletion of endogenous AHNAK.

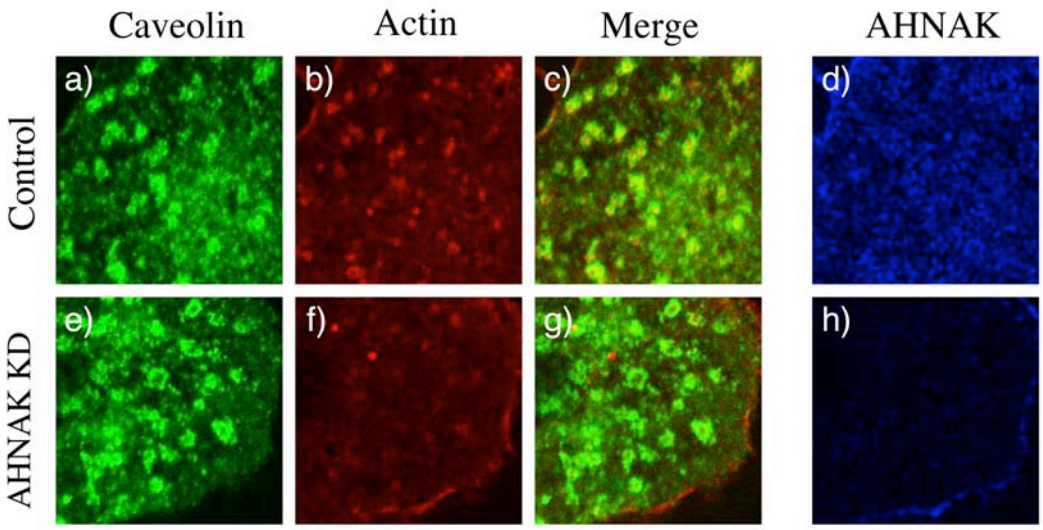

Figure 3.11. Depletion of AHNAK disrupts Cav-actin formation. Mature adipocytes were transfected with 2 nM of either random siRNA or AHNAK-specific siRNA. 72 hours after transfection, cells were fixed, permeabilized and labeled using rhodamine-conjugated phalloidin, anti-caveolin 2 and anti-AHNAK antibodies. Alexa green and blue-fluorophore conjugated secondary antibodies were use to visualize caveolin-2 and AHNAK. Images were taken by focusing at the adherent surface of representative cells to visualize the caveolar rosette formations.

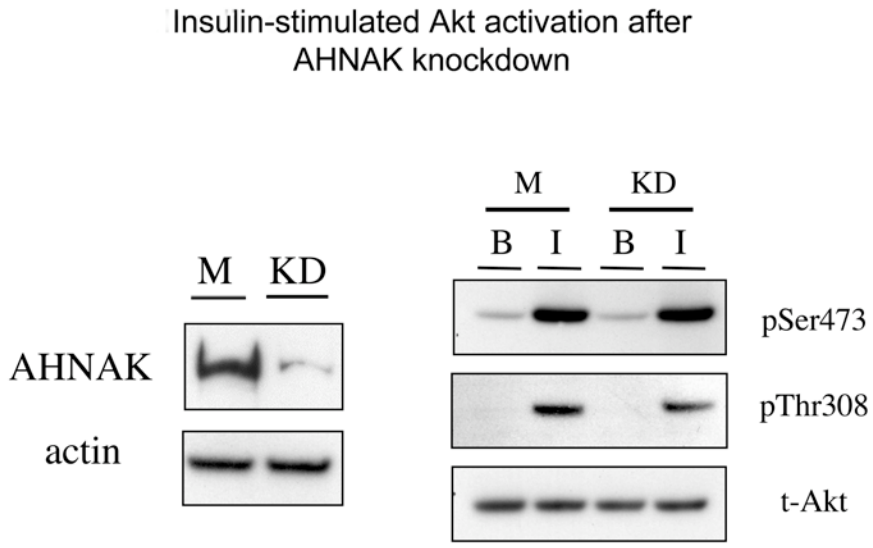

Figure 3.12. AHNAK depletion does not affect insulin-mediated Akt activation. Mature adipocytes were electroporated with 2 nmol of scramble (M-mock condition) or AHNAK-specific siRNA (KD-knockdown). On the 60th hour post-transfection, cells were shifted into serum-starving media for 12 hours. The cells were then stimulated with vehicle (B-basal) or 10 nM of insulin (I-insulin) for 20 minutes. Whole cell lysates were collected and 30 mg of total protein per condition were resolved by SDS-PAGE. a) Lysates from basal condition were immunoblotted for AHNAK and actin to confirm specific knockdown by siRNA. b) Lysates from basal and insulin stimulated conditions were immunoblotted for total Akt and phosphorylated Akt (serine 473 and threonine 308).

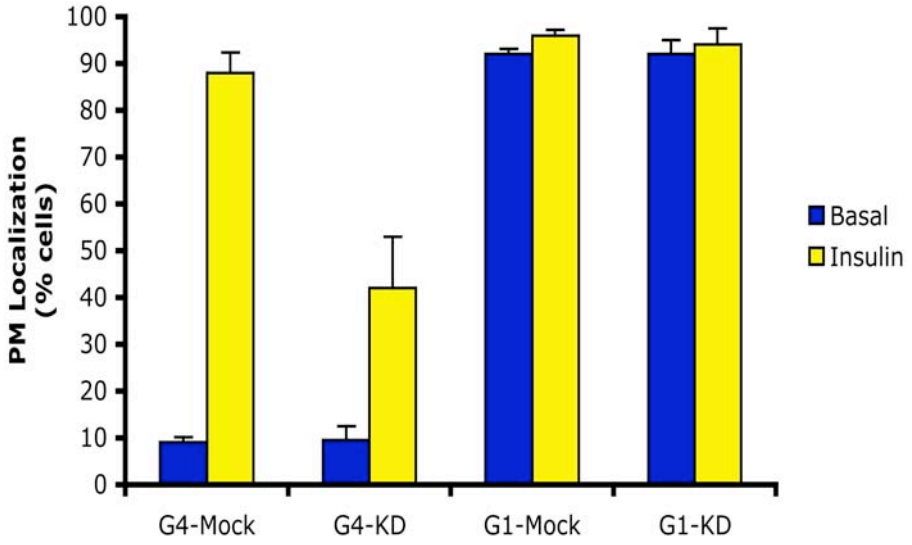

Figure 3.13. AHNAK downregulation inhibits insulin-stimulated GLUT4 translocation. Fully differentiated 3T3-L1 adipocytes were electroporated with 50 mg of myc-GLUT4-eGFP or myc-GLUT1-eGFP cDNA plus 2 nmol of scramble or AHNAK-specific siRNA. 72 hours later, the cells were stimulated with vehicle or 100 nM insulin for 20 minutes and processed for immunofluorescent microscopy. 50 cells per condition were counted for the presence of a plasma membrane GFP rim. The data presented is equivalent to the average ± SD of three independent experiments

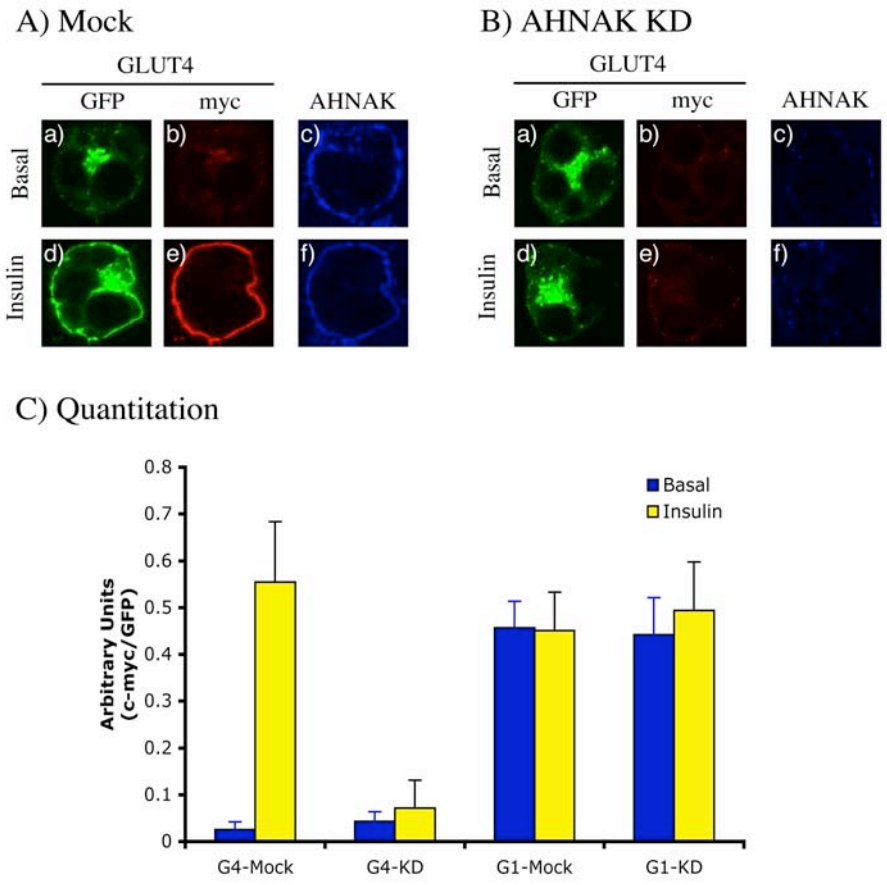

Figure 3.14. Single cell quantitation of GLUT4 translocation after AHNAK depletion. Fully differentiated adipocytes were electroporated with 50 mg of myc-GLUT4-eGFP or myc-GLUT1-eGFP cDNA plus 2 nmol of scramble or AHNAK-specific siRNA. 72 hours later, the cells were stimulated with vehicle or 100 nM insulin for 20 minutes and processed for single cell immunofluorescent microscopy. A) Representative images of control cells selected for quantitation. B) Representative images of AHNAK-depleted cells selected for quantitation. C) 15 cells per condition were evaluated using the Zeiss LSM510 software to compute for the ratio of plasma membrane myc signal over total GFP signal. The data presented is equivalent to the average ± SD of three independent experiments

CHAPTER 4
CONCLUSIONS

The vasopressin-regulated translocation of AQP2 in renal epithelial cells and the insulin-regulated exocytosis of GLUT4 in muscle and adipose tissue are supported by fundamentally different molecular machineries.

Spatial segregation of GLUT4 and AQP2 in specialized, insulin or cAMP-responsive compartments represents one central aspect of hormone regulated exocytosis. The identification of identical putative trafficking signals in GLUT4 and AQP2 suggested that regulated translocation of both proteins may be facilitated by the same basic molecular effectors operating in different cellular contexts. Using the 3T3-L1 adipocyte cell system, the study presented provides compelling evidence to argue against this hypothesis.

Sorting signals in proteins direct peptide molecules to the appropriate cellular address. In some cases, protein signals lie in a discrete stretch of amino acid sequence that will direct a protein to a specific destination in the cell. Some established signal sequences include those that direct import and export from the nucleus and import and return to the ER. A more complicated variety of sorting signal involves a specific three-dimensional arrangement of atoms on the surface of a properly folded protein. The amino acids that comprise a signal patch may be distant from one another based on the primary structure of a protein.

A reasonable approach to test whether there is functional overlap between the reported dileucine and phenylalanine-based sorting motifs in GLUT4 and AQP2 is to directly compare the trafficking of the two transporters in an adequate cell system. When AQP2 and GLUT4 were co-expressed in adipocytes, the

proteins were partitioned in separate compartments that were uniquely responsive to either insulin or forskolin. Temporally, newly-synthesized AQP2 gained direct access to the cAMP-responsive compartment sooner than it took newly-synthesized GLUT4 to enter the insulin-responsive compartment. Furthermore, unlike GLUT4, the exit of AQP2 from the TGN was independent of GGA. Collectively, these differences in biosynthetic sorting and processing suggest that regulated trafficking of GLUT4 and AQP2 are naturally facilitated by non-identical molecular machineries. The functions of the LL and phenyalanine-based motifs, if any, are most likely unique for each protein transporter. In theory, this could be achieved if each motif functions as part of different signaling patches, allowing identical motifs to subserve incongruent roles in directing the trafficking of GLUT4 and AQP2.

Finally, although adipocytes do not express AQP2, the segregation of the water channel in a cAMP-responsive compartment when overexpressed curiously suggest that adipocytes naturally support the cAMP-regulated trafficking of an unknown molecule. A possible candidate from the aquaporin family is AQP7, a glycerol channel expressed in adipose tissue. Unfortunately, a preliminary study looking at the subcellular localization of AQP7 by immunofluorescent microscopy revealed that the protein defaults to the plasma membrane. A more extensive review of available literature did not lead to any known adipokine or membrane protein in adipocyte that is secreted or translocated in response to increases in intracellular cAMP. Thus, it will be interesting to perform a proteomic analyses of the cAMP-responsive compartment using AQP2 as a marker and as a tool for isolation.

AHNAK is a molecular scaffold in adipocytes that anchors cortical F-actin to the plasma membrane at sites of caveolar formation.

The cellular cytoskeletal network is an essential component of various trafficking systems that support the movement of cargo-loaded vesicles to and from the plasma membrane (14). In the context of glucose uptake in muscle and adipose tissue, both the actin and microtubule-based cytoskeleton has been shown to play a role in the regulated exocytosis of the facilitative glucose transporter GLUT4 (5, 8, 12). In non-stimulated states, GLUT4 is effectively retained in intracellular storage compartments that are primarily composed of small transport vesicles dispersed beneath the plasma membrane (3, 6). Cytoskeleton perturbing reagents such as latrunculin and nocodazole disrupt the trafficking of these storage vesicles and impair insulin-stimulated GLUT4 exocytosis, suggesting that the cytoskeleton is crucial for the maintenance and retention of GLUT4-bearing compartments (4, 13). Additionally, insulin-induced dynamic rearrangement of filamentous actin is necessary for re-routing GLUT4 to the plasma membrane (11). This remodeling is likely mediated by two downstream effectors of insulin signaling, phosphatidylinositol 3-kinase (PI3K) and the Rho-family small GTP-binding protein TC10 (8). PI3K, by altering the phosphoinositide composition of the plasma membrane, may facilitate the recruitment and activation of known actin regulators such as the ARF family proteins (2). The caveolae-restricted TC10, on the other hand, can bind several potential effectors including the neural Wiscott-Aldrich syndrome protein (N-WASP) and atypical protein kinase C (aPKC λ/ζ), both of which are directly involved in the regulation of the actin cytoskeleton in various cell types (7, 9, 15).

In adipocytes, the plasma membrane association of AHNAK was restricted to the caveolin-enriched rosettes structures that are composed of multiple individual caveolae that are spatially organized into large ring-like structures (16).

These large domains appear to be focal sites of cortical F-actin attachment to the plasma membrane and are conceptually and perhaps functionally related to focal adhesion sites in fibroblasts (10). The association of AHNAK with these structures appears to be of relatively low affinity as AHNAK was readily released following sonication or cell homogenization but could be preserved following paraformaldehyde cross linking. Although it was reported that AHNAK is a specific marker for a unique population of vesicles called enlargeosomes that may be involved in cell differentiation and membrane repair in PC12 cells (1), the data is more consistent with AHNAK having a propensity to interact with lipidogenous membranes which allow it to associate with various intracellular membrane-bound vesicles when released from lipid raft microdomains. As in MDCK cells therefore, AHNAK in adipocyte is likely functioning as part of the molecular machinery that supports the characteristic cytoarchitecture of the mature adipocyte.

In this regard, depolymerization of cortical actin had no significant effect on the formation of caveolin-enriched rosette structures nor the association of AHNAK with caveolae, indicating that AHNAK localization is not dependent on F-actin. In contrast, disruption of the caveolin-enriched rosettes by cholesterol depletion resulted in a near complete loss of AHNAK from the plasma membrane and subsequent association with intracellular membrane-bound, vesicular compartments. Thus, the caveolin-enriched rosettes provide the necessary interactions sites for the association of AHNAK with the plasma membrane. In addition, siRNA reduction of AHNAK protein resulted in the loss of cortical F-actin organization without affecting the total amount of monomeric actin protein in the cells. The simplest model that accounts for these finding is that AHNAK provides a scaffolding function linking, either directly or indirectly, the caveolin-enriched rosettes with F-actin thereby generating the Cav-actin structures.

Several problems were encountered in determining the effect of insulin-stimulation on AHNAK in adipocytes. In terms of phosphorylation, the available

phospho-specific antibody, designed against human AHNAK, did not react consistently with endogenous AHNAK from 3T3-L1 adipocytes. Although it was clear from immunoblotting with the phospho-AHNAK antibody that there is basal phosphorylation of the protein, the effect of insulin stimulation has not been consistent. Additionally, insulin stimulation seemed to result to fragmentation or degradation of endogenous AHNAK, based on the immunoblot of total AHNAK. This precludes conclusive evaluation of changes in level of phosphorylation of AHNAK with insulin-stimulation. Alternative approaches using a custom-made phospho-specific antibody against mouse AHNAK will be essential to further investigate whether AHNAK is a downstream Akt effector in adipocytes.

REFERENCES

1. **Ahmed Z, Smith BJ, and Pillay TS.** The APS adapter protein couples the insulin receptor to the phosphorylation of c-Cbl and facilitates ligand-stimulated ubiquitination of the insulin receptor. *FEBS Lett* 475: 31-34, 2000.

2. **Al-Hasani H, Kunamneni RK, Dawson K, Hinck CS, Muller-Wieland D, and Cushman SW.** Roles of the N- and C-termini of GLUT4 in endocytosis. *J Cell Sci* 115: 131-140, 2002.

3. **Bandyopadhyay G, Kanoh Y, Sajan MP, Standaert ML, and Farese RV.** Effects of adenoviral gene transfer of wild-type, constitutively active, and kinase-defective protein kinase C-lambda on insulin-stimulated glucose transport in L6 myotubes. *Endocrinology* 141: 4120-4127, 2000.

4. **Bandyopadhyay G, Standaert ML, Galloway L, Moscat J, and Farese RV.** Evidence for involvement of protein kinase C (PKC)-zeta and noninvolvement of diacylglycerol-sensitive PKCs in insulin-stimulated glucose transport in L6 myotubes. *Endocrinology* 138: 4721-4731, 1997.

5. **Bandyopadhyay G, Standaert ML, Zhao L, Yu B, Avignon A, Galloway L, Karnam P, Moscat J, and Farese RV.** Activation of protein kinase C (alpha, beta, and zeta) by insulin in 3T3/L1 cells. Transfection studies suggest a role for PKC-zeta in glucose transport. *J Biol Chem* 272: 2551-2558, 1997.

6. **Benaud C, Gentil BJ, Assard N, Court M, Garin J, Delphin C, and Baudier J.** AHNAK interaction with the annexin 2/S100A10 complex regulates cell membrane cytoarchitecture. *J Cell Biol* 164: 133-144, 2004.

7. **Berwick DC, Dell GC, Welsh GI, Heesom KJ, Hers I, Fletcher LM, Cooke FT, and Tavare JM.** Protein kinase B phosphorylation of PIKfyve

regulates the trafficking of GLUT4 vesicles. *J Cell Sci* 117: 5985-5993, 2004.

8. **Borgonovo B, Cocucci E, Racchetti G, Podini P, Bachi A, and Meldolesi J.** Regulated exocytosis: a novel, widely expressed system. *Nat Cell Biol* 4: 955-962, 2002.

9. **Bose A, Cherniack AD, Langille SE, Nicoloro SM, Buxton JM, Park JG, Chawla A, and Czech MP.** G(alpha)11 signaling through ARF6 regulates F-actin mobilization and GLUT4 glucose transporter translocation to the plasma membrane. *Mol Cell Biol* 21: 5262-5275, 2001.

10. **Bouley R, Breton S, Sun T, McLaughlin M, Nsumu NN, Lin HY, Ausiello DA, and Brown D.** Nitric oxide and atrial natriuretic factor stimulate cGMP-dependent membrane insertion of aquaporin 2 in renal epithelial cells. *J Clin Invest* 106: 1115-1126, 2000.

11. **Brazil DP and Hemmings BA.** Ten years of protein kinase B signalling: a hard Akt to follow. *Trends Biochem Sci* 26: 657-664, 2001.

12. **Brazil DP, Park J, and Hemmings BA.** PKB binding proteins. Getting in on the Akt. *Cell* 111: 293-303, 2002.

13. **Brown D.** The ins and outs of aquaporin-2 trafficking. *Am J Physiol Renal Physiol* 284: F893-901, 2003.

14. **Brozinick JT, Jr., Hawkins ED, Strawbridge AB, and Elmendorf JS.** Disruption of cortical actin in skeletal muscle demonstrates an essential role of the cytoskeleton in glucose transporter 4 translocation in insulin-sensitive tissues. *J Biol Chem* 279: 40699-40706, 2004.

15. **Bryant NJ, Govers R, and James DE.** Regulated transport of the glucose transporter GLUT4. *Nat Rev Mol Cell Biol* 3: 267-277, 2002.

16. **Cantley LC.** The phosphoinositide 3-kinase pathway. *Science* 296: 1655-1657, 2002.

17. **Chamberlain LH and Gould GW.** The vesicle- and target-SNARE proteins that mediate Glut4 vesicle fusion are localized in detergent-insoluble lipid rafts present on distinct intracellular membranes. *J Biol Chem* 277: 49750-49754, 2002.

18. **Chiang SH, Baumann CA, Kanzaki M, Thurmond DC, Watson RT, Neudauer CL, Macara IG, Pessin JE, and Saltiel AR.** Insulin-stimulated GLUT4 translocation requires the CAP-dependent activation of TC10. *Nature* 410: 944-948, 2001.

19. **Cocucci E, Racchetti G, Podini P, Rupnik M, and Meldolesi J.** Enlargeosome, an exocytic vesicle resistant to nonionic detergents, undergoes endocytosis via a nonacidic route. *Mol Biol Cell* 15: 5356-5368, 2004.

20. **Couet J, Sargiacomo M, and Lisanti MP.** Interaction of a receptor tyrosine kinase, EGF-R, with caveolins. Caveolin binding negatively regulates tyrosine and serine/threonine kinase activities. *J Biol Chem* 272: 30429-30438, 1997.

21. **De Seranno S, Benaud C, Assard N, Khediri S, Gerke V, Baudier J, and Delphin C.** Identification of an AHNAK binding motif specific for the Annexin2/S100A10 tetramer. *J Biol Chem* 281: 35030-35038, 2006.

22. **Fushimi K, Sasaki S, and Marumo F.** Phosphorylation of serine 256 is required for cAMP-dependent regulatory exocytosis of the aquaporin-2 water channel. *J Biol Chem* 272: 14800-14804, 1997.

23. **Gentil BJ, Delphin C, Benaud C, and Baudier J.** Expression of the giant protein AHNAK (desmoyokin) in muscle and lining epithelial cells. *J Histochem Cytochem* 51: 339-348, 2003.

24. **Gonzalez E and McGraw TE.** Insulin signaling diverges into Akt-dependent and -independent signals to regulate the recruitment/docking and the fusion of GLUT4 vesicles to the plasma membrane. *Mol Biol Cell* 17: 4484-4493, 2006.

25. **Gustafson CE, Katsura T, McKee M, Bouley R, Casanova JE, and Brown D.** Recycling of AQP2 occurs through a temperature- and

bafilomycin-sensitive trans-Golgi-associated compartment. *Am J Physiol Renal Physiol* 278: F317-326, 2000.

26. **Gustavsson J, Parpal S, Karlsson M, Ramsing C, Thorn H, Borg M, Lindroth M, Peterson KH, Magnusson KE, and Stralfors P.** Localization of the insulin receptor in caveolae of adipocyte plasma membrane. *Faseb J* 13: 1961-1971, 1999.

27. **Haase H.** Ahnak, a new player in beta-adrenergic regulation of the cardiac L-type Ca2+ channel. *Cardiovasc Res* 73: 19-25, 2007.

28. **Hashiramoto M and James DE.** Characterization of insulin-responsive GLUT4 storage vesicles isolated from 3T3-L1 adipocytes. *Mol Cell Biol* 20: 416-427, 2000.

29. **Henn V, Edemir B, Stefan E, Wiesner B, Lorenz D, Theilig F, Schmitt R, Vossebein L, Tamma G, Beyermann M, Krause E, Herberg FW, Valenti G, Bachmann S, Rosenthal W, and Klussmann E.** Identification of a novel A-kinase anchoring protein 18 isoform and evidence for its role in the vasopressin-induced aquaporin-2 shuttle in renal principal cells. *J Biol Chem* 279: 26654-26665, 2004.

30. **Huang J, Hsia SH, Imamura T, Usui I, and Olefsky JM.** Annexin II is a thiazolidinedione-responsive gene involved in insulin-induced glucose transporter isoform 4 translocation in 3T3-L1 adipocytes. *Endocrinology* 145: 1579-1586, 2004.

31. **Huang J, Imamura T, Babendure JL, Lu JC, and Olefsky JM.** Disruption of microtubules ablates the specificity of insulin signaling to GLUT4 translocation in 3T3-L1 adipocytes. *J Biol Chem* 280: 42300-42306, 2005.

32. **Huang J, Imamura T, and Olefsky JM.** Insulin can regulate GLUT4 internalization by signaling to Rab5 and the motor protein dynein. *Proc Natl Acad Sci U S A* 98: 13084-13089, 2001.

33. **Huang S, Lifshitz LM, Jones C, Bellve KD, Standley C, Fonseca S, Corvera S, Fogarty KE, and Czech MP.** Insulin Stimulates Membrane

Fusion and GLUT4 Accumulation in Clathrin Coats on Adipocyte Plasma Membranes. *Mol Cell Biol* 27: 3456-3469, 2007.

34. **Hubbard SR.** Crystal structure of the activated insulin receptor tyrosine kinase in complex with peptide substrate and ATP analog. *Embo J* 16: 5572-5581, 1997.

35. **Inoue M, Chiang SH, Chang L, Chen XW, and Saltiel AR.** Compartmentalization of the exocyst complex in lipid rafts controls Glut4 vesicle tethering. *Mol Biol Cell* 17: 2303-2311, 2006.

36. **Ishii K, Hayashi H, Todaka M, Kamohara S, Kanai F, Jinnouchi H, Wang L, and Ebina Y.** Possible domains responsible for intracellular targeting and insulin-dependent translocation of glucose transporter type 4. *Biochem J* 309 (Pt 3): 813-823, 1995.

37. **Ishikawa Y, Yuan Z, Inoue N, Skowronski MT, Nakae Y, Shono M, Cho G, Yasui M, Agre P, and Nielsen S.** Identification of AQP5 in lipid rafts and its translocation to apical membranes by activation of M3 mAChRs in interlobular ducts of rat parotid gland. *Am J Physiol Cell Physiol* 289: C1303-1311, 2005.

38. **Iwanishi M, Haruta T, Takata Y, Ishibashi O, Sasaoka T, Egawa K, Imamura T, Naitou K, Itazu T, and Kobayashi M.** A mutation (Trp1193-->Leu1193) in the tyrosine kinase domain of the insulin receptor associated with type A syndrome of insulin resistance. *Diabetologia* 36: 414-422, 1993.

39. **Jablonski EM and Hughes FM, Jr.** The potential role of caveolin-1 in inhibition of aquaporins during the AVD. *Biol Cell* 98: 33-42, 2006.

40. **Jhun BH, Rampal AL, Liu H, Lachaal M, and Jung CY.** Effects of insulin on steady state kinetics of GLUT4 subcellular distribution in rat adipocytes. Evidence of constitutive GLUT4 recycling. *J Biol Chem* 267: 17710-17715, 1992.

41. **Jiang T, Sweeney G, Rudolf MT, Klip A, Traynor-Kaplan A, and Tsien RY.** Membrane-permeant esters of phosphatidylinositol 3,4,5-trisphosphate. *J Biol Chem* 273: 11017-11024, 1998.

42. **Jiang ZY, Chawla A, Bose A, Way M, and Czech MP.** A phosphatidylinositol 3-kinase-independent insulin signaling pathway to N-WASP/Arp2/3/F-actin required for GLUT4 glucose transporter recycling. *J Biol Chem* 277: 509-515, 2002.

43. **Jiang ZY, Zhou QL, Coleman KA, Chouinard M, Boese Q, and Czech MP.** Insulin signaling through Akt/protein kinase B analyzed by small interfering RNA-mediated gene silencing. *Proc Natl Acad Sci U S A* 100: 7569-7574, 2003.

44. **Jo I, Ward DT, Baum MA, Scott JD, Coghlan VM, Hammond TG, and Harris HW.** AQP2 is a substrate for endogenous PP2B activity within an inner medullary AKAP-signaling complex. *Am J Physiol Renal Physiol* 281: F958-965, 2001.

45. **Kamsteeg EJ, Heijnen I, van Os CH, and Deen PM.** The subcellular localization of an aquaporin-2 tetramer depends on the stoichiometry of phosphorylated and nonphosphorylated monomers. *J Cell Biol* 151: 919-930, 2000.

46. **Kanzaki M.** Insulin receptor signals regulating GLUT4 translocation and actin dynamics. *Endocr J* 53: 267-293, 2006.

47. **Kanzaki M, Furukawa M, Raab W, and Pessin JE.** Phosphatidylinositol 4,5-bisphosphate regulates adipocyte actin dynamics and GLUT4 vesicle recycling. *J Biol Chem* 279: 30622-30633, 2004.

48. **Kanzaki M, Mora S, Hwang JB, Saltiel AR, and Pessin JE.** Atypical protein kinase C (PKCzeta/lambda) is a convergent downstream target of the insulin-stimulated phosphatidylinositol 3-kinase and TC10 signaling pathways. *J Cell Biol* 164: 279-290, 2004.

49. **Kanzaki M and Pessin JE.** Caveolin-associated filamentous actin (Cav-actin) defines a novel F-actin structure in adipocytes. *J Biol Chem* 277: 25867-25869, 2002.

50. **Kanzaki M and Pessin JE.** Insulin-stimulated GLUT4 translocation in adipocytes is dependent upon cortical actin remodeling. *J Biol Chem* 276: 42436-42444, 2001.

51. **Kanzaki M, Watson RT, Khan AH, and Pessin JE.** Insulin stimulates actin comet tails on intracellular GLUT4-containing compartments in differentiated 3T3L1 adipocytes. *J Biol Chem* 276: 49331-49336, 2001.

52. **Kao AW, Ceresa BP, Santeler SR, and Pessin JE.** Expression of a dominant interfering dynamin mutant in 3T3L1 adipocytes inhibits GLUT4 endocytosis without affecting insulin signaling. *J Biol Chem* 273: 25450-25457, 1998.

53. **Katsura T, Ausiello DA, and Brown D.** Direct demonstration of aquaporin-2 water channel recycling in stably transfected LLC-PK1 epithelial cells. *Am J Physiol* 270: F548-553, 1996.

54. **Katsura T, Gustafson CE, Ausiello DA, and Brown D.** Protein kinase A phosphorylation is involved in regulated exocytosis of aquaporin-2 in transfected LLC-PK1 cells. *Am J Physiol* 272: F817-822, 1997.

55. **Khan AH, Capilla E, Hou JC, Watson RT, Smith JR, and Pessin JE.** Entry of newly synthesized GLUT4 into the insulin-responsive storage compartment is dependent upon both the amino terminus and the large cytoplasmic loop. *J Biol Chem* 279: 37505-37511, 2004.

56. **Kido Y, Burks DJ, Withers D, Bruning JC, Kahn CR, White MF, and Accili D.** Tissue-specific insulin resistance in mice with mutations in the insulin receptor, IRS-1, and IRS-2. *J Clin Invest* 105: 199-205, 2000.

57. **Klussmann E, Maric K, Wiesner B, Beyermann M, and Rosenthal W.** Protein kinase A anchoring proteins are required for vasopressin-mediated translocation of aquaporin-2 into cell membranes of renal principal cells. *J Biol Chem* 274: 4934-4938, 1999.

58. **Klussmann E, Tamma G, Lorenz D, Wiesner B, Maric K, Hofmann F, Aktories K, Valenti G, and Rosenthal W.** An inhibitory role of Rho in the vasopressin-mediated translocation of aquaporin-2 into cell membranes of renal principal cells. *J Biol Chem* 276: 20451-20457, 2001.

59. **Kohn AD, Summers SA, Birnbaum MJ, and Roth RA.** Expression of a constitutively active Akt Ser/Thr kinase in 3T3-L1 adipocytes stimulates

glucose uptake and glucose transporter 4 translocation. *J Biol Chem* 271: 31372-31378, 1996.

60. **Kupriyanova TA, Kandror V, and Kandror KV.** Isolation and characterization of the two major intracellular Glut4 storage compartments. *J Biol Chem* 277: 9133-9138, 2002.

61. **Lai EC.** Lipid rafts make for slippery platforms. *J Cell Biol* 162: 365-370, 2003.

62. **Lande MB, Jo I, Zeidel ML, Somers M, and Harris HW, Jr.** Phosphorylation of aquaporin-2 does not alter the membrane water permeability of rat papillary water channel-containing vesicles. *J Biol Chem* 271: 5552-5557, 1996.

63. **Larance M, Ramm G, Stockli J, van Dam EM, Winata S, Wasinger V, Simpson F, Graham M, Junutula JR, Guilhaus M, and James DE.** Characterization of the role of the Rab GTPase-activating protein AS160 in insulin-regulated GLUT4 trafficking. *J Biol Chem* 280: 37803-37813, 2005.

64. **Lawlor MA and Alessi DR.** PKB/Akt: a key mediator of cell proliferation, survival and insulin responses? *J Cell Sci* 114: 2903-2910, 2001.

65. **Lee H, Woodman SE, Engelman JA, Volonte D, Galbiati F, Kaufman HL, Lublin DM, and Lisanti MP.** Palmitoylation of caveolin-1 at a single site (Cys-156) controls its coupling to the c-Src tyrosine kinase: targeting of dually acylated molecules (GPI-linked, transmembrane, or cytoplasmic) to caveolae effectively uncouples c-Src and caveolin-1 (TYR-14). *J Biol Chem* 276: 35150-35158, 2001.

66. **Liu J, Kimura A, Baumann CA, and Saltiel AR.** APS facilitates c-Cbl tyrosine phosphorylation and GLUT4 translocation in response to insulin in 3T3-L1 adipocytes. *Mol Cell Biol* 22: 3599-3609, 2002.

67. **Marples D, Barber B, and Taylor A.** Effect of a dynein inhibitor on vasopressin action in toad urinary bladder. *J Physiol* 490 (Pt 3): 767-774, 1996.

68. **Marples D, Schroer TA, Ahrens N, Taylor A, Knepper MA, and Nielsen S.** Dynein and dynactin colocalize with AQP2 water channels in intracellular vesicles from kidney collecting duct. *Am J Physiol* 274: F384-394, 1998.

69. **Mazzone A, Tietz P, Jefferson J, Pagano R, and LaRusso NF.** Isolation and characterization of lipid microdomains from apical and basolateral plasma membranes of rat hepatocytes. *Hepatology* 43: 287-296, 2006.

70. **Melvin DR, Marsh BJ, Walmsley AR, James DE, and Gould GW.** Analysis of amino and carboxy terminal GLUT-4 targeting motifs in 3T3-L1 adipocytes using an endosomal ablation technique. *Biochemistry* 38: 1456-1462, 1999.

71. **Miinea CP, Sano H, Kane S, Sano E, Fukuda M, Peranen J, Lane WS, and Lienhard GE.** AS160, the Akt substrate regulating GLUT4 translocation, has a functional Rab GTPase-activating protein domain. *Biochem J* 391: 87-93, 2005.

72. **Moller DE, Yokota A, Ginsberg-Fellner F, and Flier JS.** Functional properties of a naturally occurring Trp1200----Ser1200 mutation of the insulin receptor. *Mol Endocrinol* 4: 1183-1191, 1990.

73. **Nakatsu F and Ohno H.** Adaptor protein complexes as the key regulators of protein sorting in the post-Golgi network. *Cell Struct Funct* 28: 419-429, 2003.

74. **Nielsen S, Chou CL, Marples D, Christensen EI, Kishore BK, and Knepper MA.** Vasopressin increases water permeability of kidney collecting duct by inducing translocation of aquaporin-CD water channels to plasma membrane. *Proc Natl Acad Sci U S A* 92: 1013-1017, 1995.

75. **Nielsen S, Marples D, Birn H, Mohtashami M, Dalby NO, Trimble M, and Knepper M.** Expression of VAMP-2-like protein in kidney collecting duct intracellular vesicles. Colocalization with Aquaporin-2 water channels. *J Clin Invest* 96: 1834-1844, 1995.

76. **Okada S, Ohshima K, Uehara Y, Shimizu H, Hashimoto K, Yamada M, and Mori M.** Synip phosphorylation is required for insulin-stimulated Glut4 translocation. *Biochem Biophys Res Commun* 356: 102-106, 2007.

77. **Okada T, Kawano Y, Sakakibara T, Hazeki O, and Ui M.** Essential role of phosphatidylinositol 3-kinase in insulin-induced glucose transport and antilipolysis in rat adipocytes. Studies with a selective inhibitor wortmannin. *J Biol Chem* 269: 3568-3573, 1994.

78. **Olson AL, Trumbly AR, and Gibson GV.** Insulin-mediated GLUT4 translocation is dependent on the microtubule network. *J Biol Chem* 276: 10706-10714, 2001.

79. **Parpal S, Karlsson M, Thorn H, and Stralfors P.** Cholesterol depletion disrupts caveolae and insulin receptor signaling for metabolic control via insulin receptor substrate-1, but not for mitogen-activated protein kinase control. *J Biol Chem* 276: 9670-9678, 2001.

80. **Patki V, Buxton J, Chawla A, Lifshitz L, Fogarty K, Carrington W, Tuft R, and Corvera S.** Insulin action on GLUT4 traffic visualized in single 3T3-l1 adipocytes by using ultra-fast microscopy. *Mol Biol Cell* 12: 129-141, 2001.

81. **Piper RC, Tai C, Kulesza P, Pang S, Warnock D, Baenziger J, Slot JW, Geuze HJ, Puri C, and James DE.** GLUT-4 NH2 terminus contains a phenylalanine-based targeting motif that regulates intracellular sequestration. *J Cell Biol* 121: 1221-1232, 1993.

82. **Procino G, Carmosino M, Marin O, Brunati AM, Contri A, Pinna LA, Mannucci R, Nielsen S, Kwon TH, Svelto M, and Valenti G.** Ser-256 phosphorylation dynamics of Aquaporin 2 during maturation from the ER to the vesicular compartment in renal cells. *Faseb J* 17: 1886-1888, 2003.

83. **Razani B, Combs TP, Wang XB, Frank PG, Park DS, Russell RG, Li M, Tang B, Jelicks LA, Scherer PE, and Lisanti MP.** Caveolin-1-deficient mice are lean, resistant to diet-induced obesity, and show hypertriglyceridemia with adipocyte abnormalities. *J Biol Chem* 277: 8635-8647, 2002.

84. **Razani B, Rubin CS, and Lisanti MP.** Regulation of cAMP-mediated signal transduction via interaction of caveolins with the catalytic subunit of protein kinase A. *J Biol Chem* 274: 26353-26360, 1999.

85. **Sano H, Kane S, Sano E, Miinea CP, Asara JM, Lane WS, Garner CW, and Lienhard GE.** Insulin-stimulated phosphorylation of a Rab GTPase-activating protein regulates GLUT4 translocation. *J Biol Chem* 278: 14599-14602, 2003.

86. **Scheiffele P and Fullekrug J.** Glycosylation and protein transport. *Essays Biochem* 36: 27-35, 2000.

87. **Scherer PE, Lisanti MP, Baldini G, Sargiacomo M, Mastick CC, and Lodish HF.** Induction of caveolin during adipogenesis and association of GLUT4 with caveolin-rich vesicles. *J Cell Biol* 127: 1233-1243, 1994.

88. **Schnitzer JE and Oh P.** Aquaporin-1 in plasma membrane and caveolae provides mercury-sensitive water channels across lung endothelium. *Am J Physiol* 270: H416-422, 1996.

89. **Shewan AM, Marsh BJ, Melvin DR, Martin S, Gould GW, and James DE.** The cytosolic C-terminus of the glucose transporter GLUT4 contains an acidic cluster endosomal targeting motif distal to the dileucine signal. *Biochem J* 350 Pt 1: 99-107, 2000.

90. **Shisheva A, Rusin B, Ikonomov OC, DeMarco C, and Sbrissa D.** Localization and insulin-regulated relocation of phosphoinositide 5-kinase PIKfyve in 3T3-L1 adipocytes. *J Biol Chem* 276: 11859-11869, 2001.

91. **Shtivelman E, Cohen FE, and Bishop JM.** A human gene (AHNAK) encoding an unusually large protein with a 1.2-microns polyionic rod structure. *Proc Natl Acad Sci U S A* 89: 5472-5476, 1992.

92. **Soldati T and Schliwa M.** Powering membrane traffic in endocytosis and recycling. *Nat Rev Mol Cell Biol* 7: 897-908, 2006.

93. **Subtil A, Lampson MA, Keller SR, and McGraw TE.** Characterization of the insulin-regulated endocytic recycling mechanism in 3T3-L1

adipocytes using a novel reporter molecule. *J Biol Chem* 275: 4787-4795, 2000.

94. **Sun TX, Van Hoek A, Huang Y, Bouley R, McLaughlin M, and Brown D.** Aquaporin-2 localization in clathrin-coated pits: inhibition of endocytosis by dominant-negative dynamin. *Am J Physiol Renal Physiol* 282: F998-1011, 2002.

95. **Sussman J, Stokoe D, Ossina N, and Shtivelman E.** Protein kinase B phosphorylates AHNAK and regulates its subcellular localization. *J Cell Biol* 154: 1019-1030, 2001.

96. **Tajika Y, Matsuzaki T, Suzuki T, Aoki T, Hagiwara H, Kuwahara M, Sasaki S, and Takata K.** Aquaporin-2 is retrieved to the apical storage compartment via early endosomes and phosphatidylinositol 3-kinase-dependent pathway. *Endocrinology* 145: 4375-4383, 2004.

97. **Tajika Y, Matsuzaki T, Suzuki T, Aoki T, Hagiwara H, Tanaka S, Kominami E, and Takata K.** Immunohistochemical characterization of the intracellular pool of water channel aquaporin-2 in the rat kidney. *Anat Sci Int* 77: 189-195, 2002.

98. **Tamma G, Klussmann E, Maric K, Aktories K, Svelto M, Rosenthal W, and Valenti G.** Rho inhibits cAMP-induced translocation of aquaporin-2 into the apical membrane of renal cells. *Am J Physiol Renal Physiol* 281: F1092-1101, 2001.

99. **Tamma G, Klussmann E, Procino G, Svelto M, Rosenthal W, and Valenti G.** cAMP-induced AQP2 translocation is associated with RhoA inhibition through RhoA phosphorylation and interaction with RhoGDI. *J Cell Sci* 116: 1519-1525, 2003.

100. **Tamma G, Wiesner B, Furkert J, Hahm D, Oksche A, Schaefer M, Valenti G, Rosenthal W, and Klussmann E.** The prostaglandin E2 analogue sulprostone antagonizes vasopressin-induced antidiuresis through activation of Rho. *J Cell Sci* 116: 3285-3294, 2003.

101. **Tang Z, Scherer PE, Okamoto T, Song K, Chu C, Kohtz DS, Nishimoto I, Lodish HF, and Lisanti MP.** Molecular cloning of

caveolin-3, a novel member of the caveolin gene family expressed predominantly in muscle. *J Biol Chem* 271: 2255-2261, 1996.

102. **Tekirian TL.** The central role of the trans-Golgi network as a gateway of the early secretory pathway: physiologic vs nonphysiologic protein transit. *Exp Cell Res* 281: 9-18, 2002.

103. **Thurmond DC, Ceresa BP, Okada S, Elmendorf JS, Coker K, and Pessin JE.** Regulation of insulin-stimulated GLUT4 translocation by Munc18c in 3T3L1 adipocytes. *J Biol Chem* 273: 33876-33883, 1998.

104. **Uberall F, Hellbert K, Kampfer S, Maly K, Villunger A, Spitaler M, Mwanjewe J, Baier-Bitterlich G, Baier G, and Grunicke HH.** Evidence that atypical protein kinase C-lambda and atypical protein kinase C-zeta participate in Ras-mediated reorganization of the F-actin cytoskeleton. *J Cell Biol* 144: 413-425, 1999.

105. **van Balkom BW, Graat MP, van Raak M, Hofman E, van der Sluijs P, and Deen PM.** Role of cytoplasmic termini in sorting and shuttling of the aquaporin-2 water channel. *Am J Physiol Cell Physiol* 286: C372-379, 2004.

106. **Van Balkom BW, Savelkoul PJ, Markovich D, Hofman E, Nielsen S, Van Der Sluijs P, and Deen PM.** The role of putative phosphorylation sites in the targeting and shuttling of the Aquaporin-2 water channel. *J Biol Chem*, 2002.

107. **van Balkom BW, Savelkoul PJ, Markovich D, Hofman E, Nielsen S, van der Sluijs P, and Deen PM.** The role of putative phosphorylation sites in the targeting and shuttling of the aquaporin-2 water channel. *J Biol Chem* 277: 41473-41479, 2002.

108. **Watson RT, Khan AH, Furukawa M, Hou JC, Li L, Kanzaki M, Okada S, Kandror KV, and Pessin JE.** Entry of newly synthesized GLUT4 into the insulin-responsive storage compartment is GGA dependent. *Embo J* 23: 2059-2070, 2004.

109. **Watson RT, Shigematsu S, Chiang SH, Mora S, Kanzaki M, Macara IG, Saltiel AR, and Pessin JE.** Lipid raft microdomain

compartmentalization of TC10 is required for insulin signaling and GLUT4 translocation. *J Cell Biol* 154: 829-840, 2001.

110. **Welsh GI, Hers I, Berwick DC, Dell G, Wherlock M, Birkin R, Leney S, and Tavare JM.** Role of protein kinase B in insulin-regulated glucose uptake. *Biochem Soc Trans* 33: 346-349, 2005.

111. **White MF.** IRS proteins and the common path to diabetes. *Am J Physiol Endocrinol Metab* 283: E413-422, 2002.

112. **White MF.** The IRS-signaling system: a network of docking proteins that mediate insulin and cytokine action. *Recent Prog Horm Res* 53: 119-138, 1998.

113. **Withers DJ, Gutierrez JS, Towery H, Burks DJ, Ren JM, Previs S, Zhang Y, Bernal D, Pons S, Shulman GI, Bonner-Weir S, and White MF.** Disruption of IRS-2 causes type 2 diabetes in mice. *Nature* 391: 900-904, 1998.

114. **Yamashita Y, Hirai K, Katayama Y, Fushimi K, Sasaki S, and Marumo F.** Mutations in sixth transmembrane domain of AQP2 inhibit its translocation induced by vasopression. *Am J Physiol Renal Physiol* 278: F395-405, 2000.

115. **Zheng X and Bollinger Bollag W.** Aquaporin 3 colocates with phospholipase d2 in caveolin-rich membrane microdomains and is downregulated upon keratinocyte differentiation. *J Invest Dermatol* 121: 1487-1495, 2003.